NASA Grant Number NAG 2-389

Thermal Analysis and Design of a Cooling System for a Mach 14 Nozzle

FINAL REPORT

covering period February, 1986 to January, 1987

Submitted to:
Thomas Polek
Chief, thermodynamics Facilities Branch
NASA Ames Research Center
Moffett Field, CA 94035

Prepared by:
Ronald Mullisen, principal investigator
Keith Kaste, graduate student
Mechanical Engineering Department
California Polytechnic State University
San Luis Obispo, CA 93407

30 January 1987

ABSTRACT

THERMAL ANALYSIS AND DESIGN OF A COOLING SYSTEM FOR THE NASA AMES MACH 14 WIND TUNNEL NOZZLE

This report provides the analysis and design of a Mach 14 converging diverging nozzle wall liner. The analysis indicates that: no fin on the coolant side of the nozzle wall is optimum, the thermal stresses are dominant, and the critical area is very near the throat. The molybdenum alloy TZM, with a wall thickness of 2.0 mm in the throat area, appears to be the only material capable of meeting design requirements. Additionally, cooling water at 2000 psia with a flow velocity of 25 m/s in the coolant passages is required.

ACKNOWLEDGEMENTS

I would like to express gratitude to my thesis advisor, Professor R. S. Mullisen, for his valuable guidance, encouragement and sense of humor. I would also like to thank the thesis committee members Professors W. E. Clark and R. G. Gordon.

This work was sponsored by NASA Ames under grant NAG 2-389. Many thanks to those at Moffett Field who made this project possible.

Finally, I would like to extend much appreciation to my wife, Gail, for her inspiration, encouragement and support during this growth period of our lives.

TABLE OF CONTENTS

TABLE OF CONTENTS (continued)

LIST OF TABLES

LIST OF FIGURES

LIST OF FIGURES (continued)

NOMENCLATURE

A	heat transfer area, m^2
C_f	skin friction coefficient, unitless
c_p	specific heat, kJ/kg·K
D_h	hydraulic diameter, m
E	modulus of elasticity, psi
h	heat transfer coefficient, $W/m^2 \cdot K$
k	thermal conductivity of liner material, W/m K
L	length, m
Ma	Mach number, unitless
Nu	Nusselt number, unitless
p	pressure, psi
P	pressure, psi
Pr	Prandtl number, unitless
q	transferred heat energy, W
r	radius, m
r	recovery factor, unitless
R	radius, m
Re	Reynolds number, unitless
S_y	yield strength, psi
St	Stanton number, unitless
T	temperature, °F, °C, Kelvin
U	velocity, m/s
V	velocity, m/s

NOMENCLATURE (continued)

w	coolant passage width, m
x	distance along nozzle wall, m
z	distance along nozzle axis of symmetry, m

SUBSCRIPTS

0	stagnation conditions
a	air side
b	bulk conditions
c	coolant side
i	inside surface
o	outside surface
st	straight
r	radial component
R	recovery
w	wall
z	axial component
∞	static conditions
*	throat conditions
θ	circumferential component

NOMENCLATURE (continued)

GREEK

α	coefficient of thermal expansion, m/m K
γ	ratio of specific heats, unitless
δ	velocity thickness, m
δ^*	displacement thickness, m
δ_p	potential boundary layer thickness, m
δ_r	real boundary layer thickness, m
Δ	temperature thickness, m
θ	temperature difference, Kelvin
θ	momentum thickness, m
λ	Poisson ratio, unitless
μ	dynamic viscosity, kg/m s
ν	kinematic viscosity, m^2/s
ρ	density, kg/m^3
σ	stress, psi
ϕ	energy thickness, m

CHAPTER 1

Introduction

In order to test large aerospace models under hypersonic conditions the 3.5 foot blowdown type wind tunnel shown in Figure 1 was designed in 1957 by NASA Ames engineers. The supply air was compressed and then heated in a gas-fired pebble-bed heater to the necessary stagnation conditions. Four interchangeable nozzles were to permit airspeeds of Mach 5, 7, 10 and 14. However, unexpected problems prevented the Mach 14 nozzle from being used.

The original Mach 14 nozzle shown in Figure 2 is taken from a NASA drawing. The converging section of the nozzle employs a water cooling system, while the diverging section uses film cooling via injection at the throat. It is desired to eliminate the film cooling and switch to a water cooling system for the diverging section as well. The nozzle is to be operated at an inlet temperature and pressure of 3460 °R and 2000 psia, respectively. The objective of this research is to design a cooling system which will allow the nozzle to operate within its material limitations.

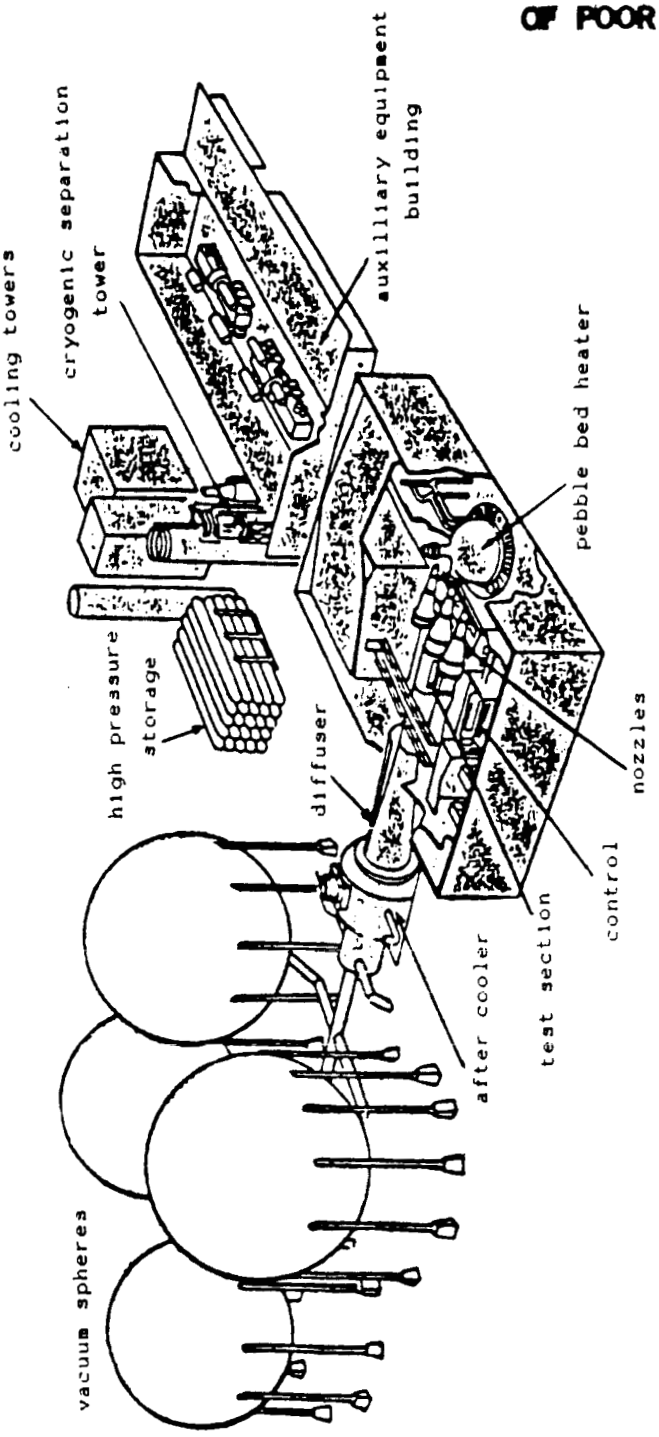

Figure 1. Components of the NASA Ames 3.5 foot hypersonic wind tunnel.

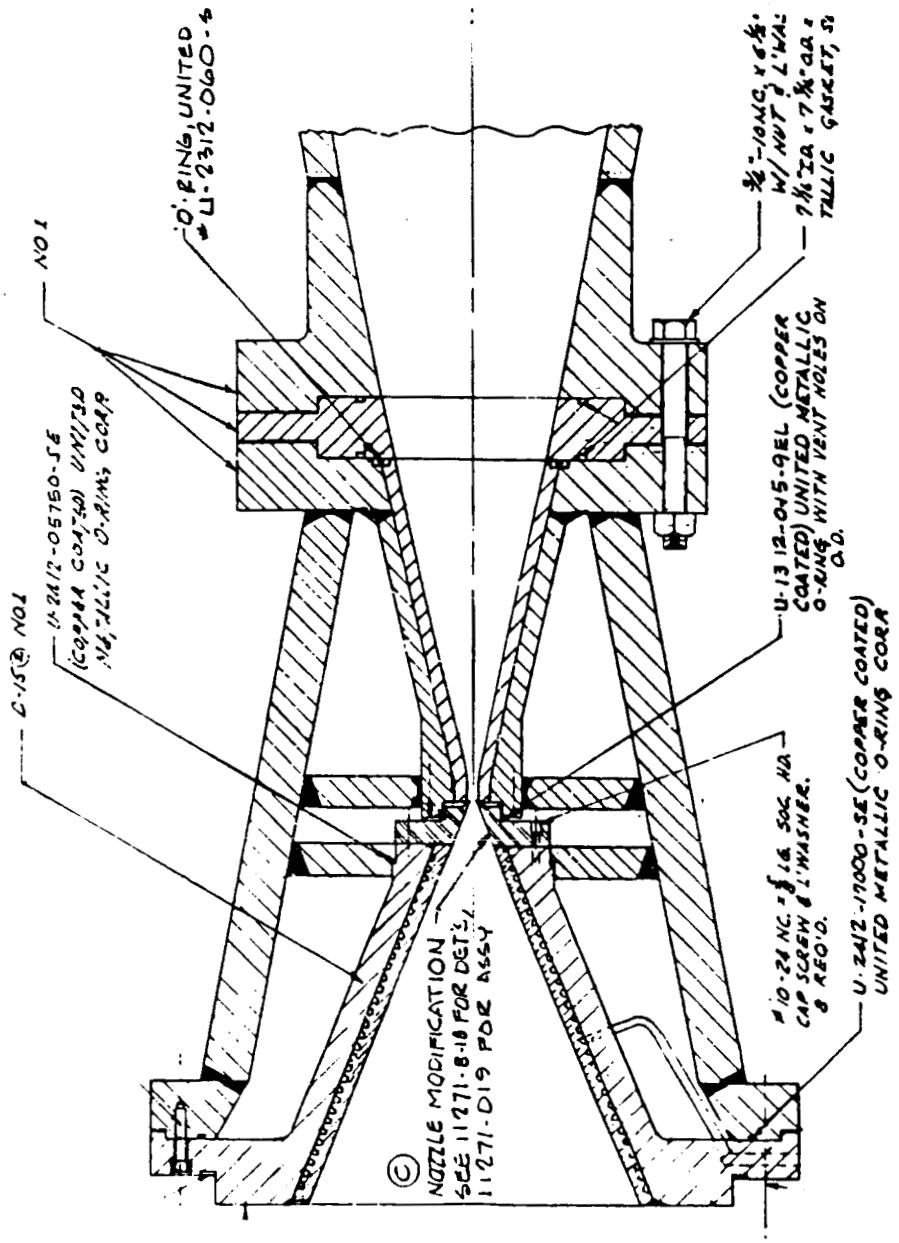

Figure 2. Cross section of original Mach 14 nozzle.

CHAPTER 2

Design

The design of the cooling system for this nozzle began with the following requirements: (1) The nozzle is fixed and is given in Figure 3. (2) The nozzle profile is supplied with dry air at 2000 psia and 3460 °R. The next requirement was the obvious necessity of having the nozzle operate within its material limitations. This encompasses two considerations: (1) The material must not exceed its oxidation temperature, and (2) the total maximum stress must not exceed the yield strength of the material at its elevated operating temperature.

Engineering design is a combination of synthesis and analysis. An initial design is analyzed and the results of this analysis lead to an improved design, which is again analyzed and improved. This process continues until an optimum design is attained.

Past experience showed that the nozzle wall must be cooled. The first design thus began with a wall finned on the backside as shown in Figure 4. The objective in this initial approach was to optimize the fin geometry (dimensions d_1 through d_4). A numerical simulation using a finite difference model of the finned wall with appropriate expressions for heat transfer coefficients on the air and coolant sides, and for a variety of wall materials, revealed that no fin was optimal! This conclusion was later

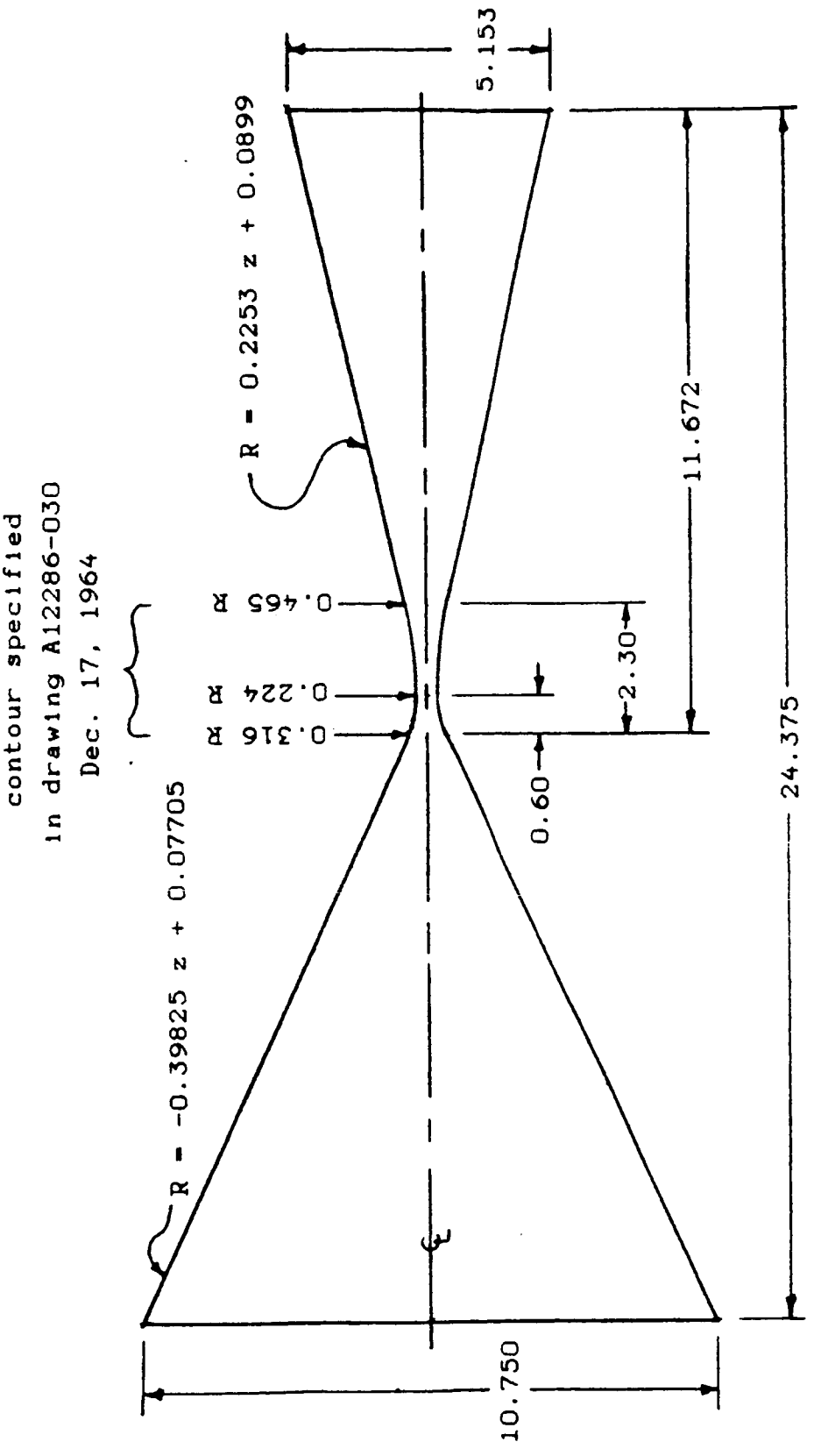

Figure 3. Mach 14 wind tunnel nozzle geometry.

confirmed with a mathematical approach involving a critical Biot number which is described in detail in Appendix A .

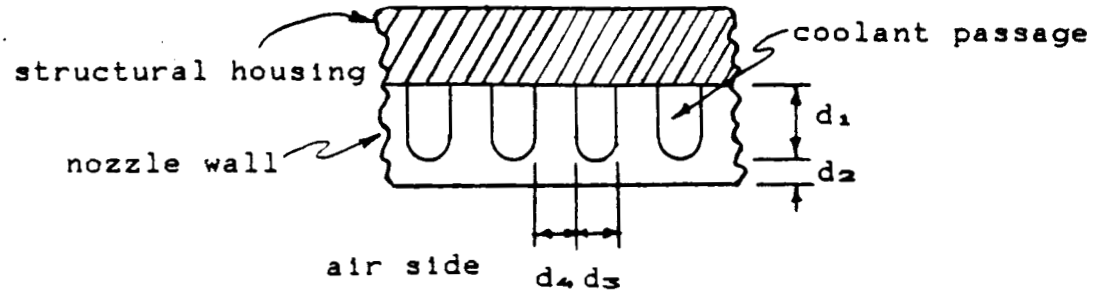

Figure 4. Initial design of nozzle wall with fins.

The analysis then focused on a plane wall as shown in Figure 5. Preliminary analysis indicated that the most critical need for cooling is in a region 5 inches upstream to 5 inches downstream of the throat. Thus the design shown in Figure 6 was finally arrived at.

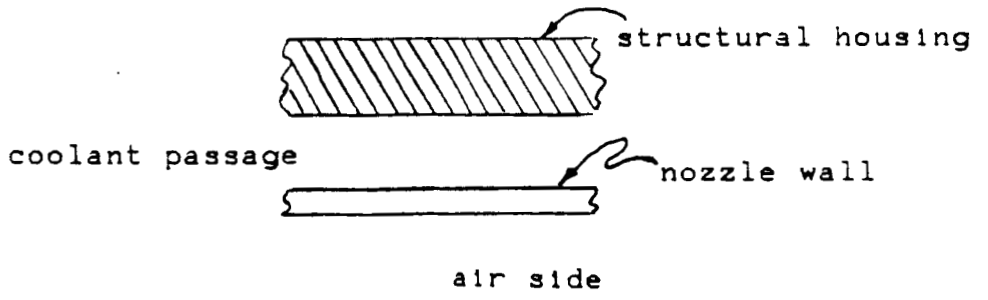

Figure 5. The plane nozzle wall.

Note that the liner contains a flanged end downstream and a sliding upstream end with a seal. This design allows for thermal expansion. The reason for having the downstream end fixed and the upstream end free is due to flow considerations. The free end will present a discontinuity in the wall profile. This discontinuity is less detrimental to the flow on the converging wall than on the diverging wall. The disadvantage associated with this arrangement is that the seal of the floating end sees air pressure at about 2000 psia and nearly 3460 °R, whereas the downstream air pressure is only about 4 psia with a temperature well below 500 °R. Thus, a special dynamic seal is required in the high temperature region.

Note the taper in the wall thickness from the throat section to either end of the nozzle liner. To facilitate heat transfer, past experience has indicated that the liner wall must be quite thin in the throat region. However, a thicker wall is more desirable at the downstream end of the nozzle for transition to the flange. Similarly, a thicker wall is more desirable at the upstream end where the dynamic seal is located.

Coolant flow is at right angles to the air flow across the backside of the nozzle liner. Channel definition is accomplished with the bosses or channel dividers shown in Figure 6. This design provides predictable heat transfer results over the entire cooled portion of the nozzle liner.

FOLDOUT FRAME

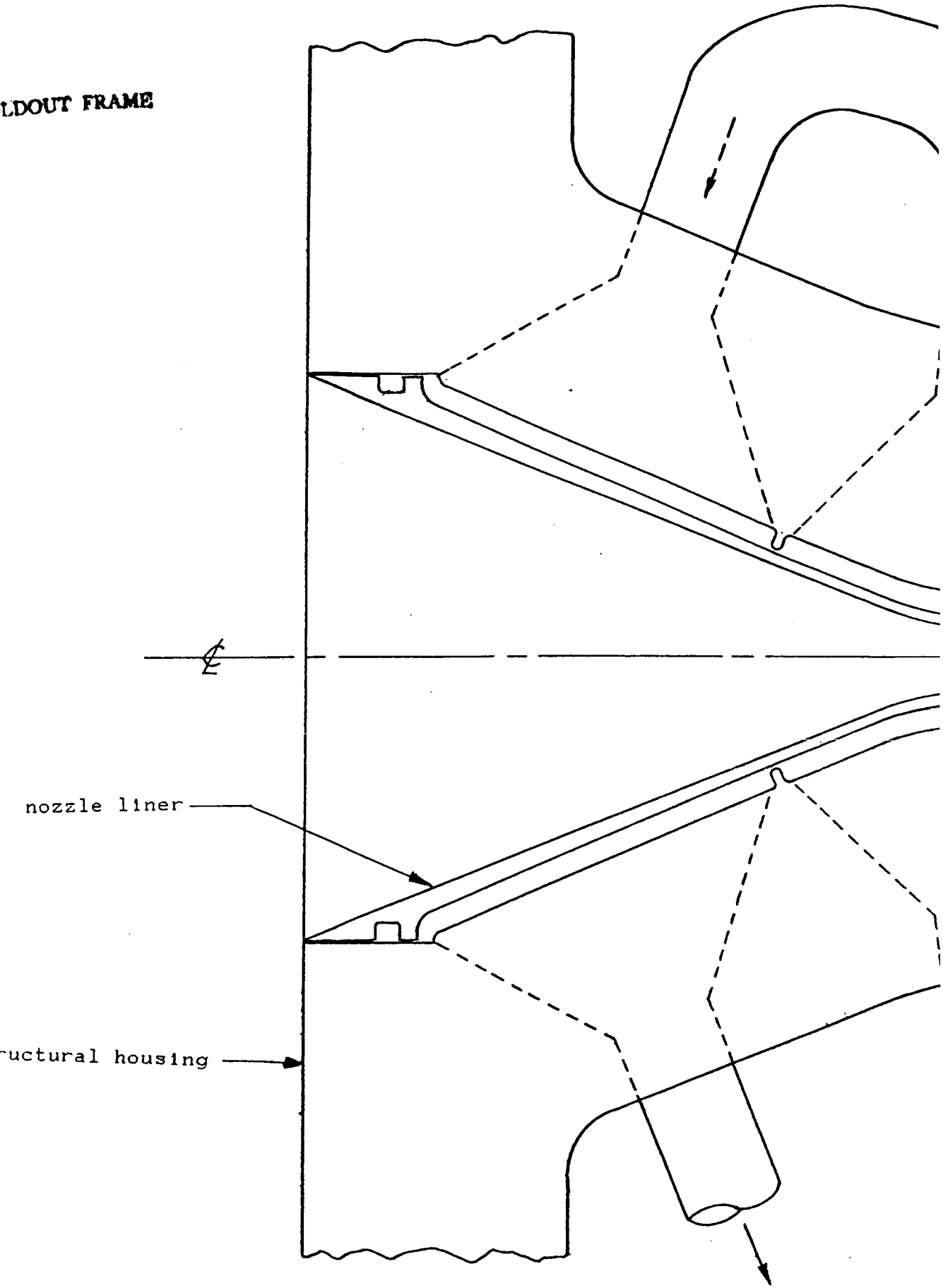

Figure 6. The proposed Mach 14 nozzle and coolant system design.

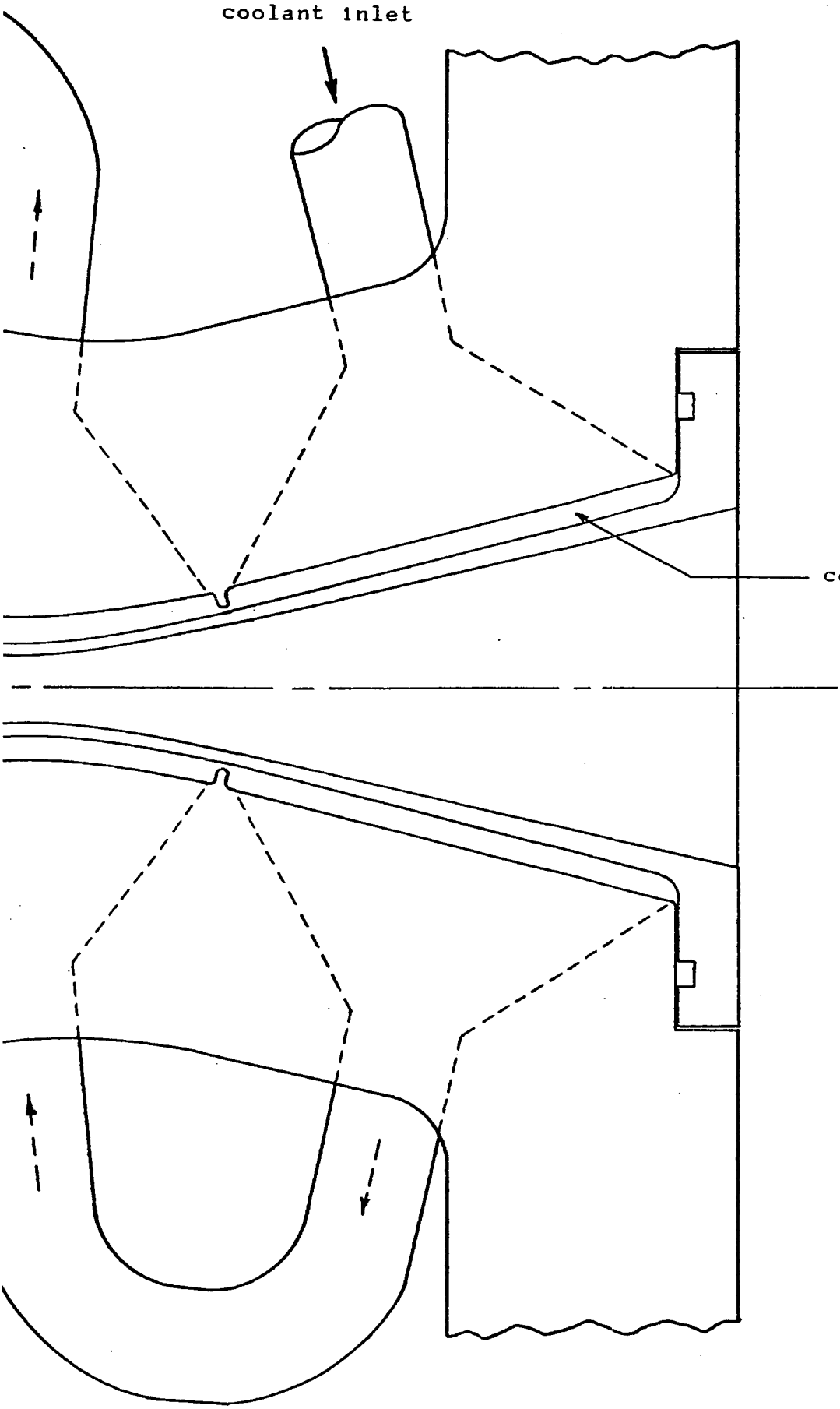

2 FOLDOUT FRAME

The coolant passages are well defined, curved rectangular ducts 0.4 cm high by approximately 8.0 cm in width.

In order to maintain a nearly constant coolant velocity throughout the cooled portion of the nozzle a series ducting system is used as shown in Figure 6. A pressure differential between the various coolant passages causes bypass coolant flow around the channel dividers thus cooling the nozzle wall in this area. High pressure, high flow rate coolant is introduced to the nozzle at the downstream section. Any rise in coolant bulk temperature will be minimal since the cooling requirement is low in this section. Next the coolant is delivered to the throat section where the majority of heat transfer takes place. The coolant then passes through the upstream flow passage and exits the nozzle section.

With the basic design of the nozzle liner established, it is now necessary to optimize the wall thickness profile, and to select an appropriate material. Additionally, the coolant must be optimized for flow rate, bulk temperature and pressure. In the following chapter we develop the analyses necessary to choose the best design parameters.

CHAPTER 3

Analysis

The analysis was performed in the following sequence:

1. Flow analysis. This gives the temperature, pressure, and Mach number throughout the nozzle.

2. Thermal analysis. In this analysis the nozzle wall temperature distribution is obtained as a function of the various design parameters.

3. Stress analysis. With the known temperature distribution thermal stresses are obtained and combined with pressure stresses.

4. Material analysis. This analysis shows the relative importance of the physical properties of the candidate materials.

Flow Analysis

Given the nozzle inlet temperature and pressure the local free stream temperature, pressure, and Mach number are obtained using compressible flow theory. Given the geometry of the nozzle we can solve for the Mach number implicitly using the Mach number relation for air ($\gamma = 1.4$)

$$\frac{A}{A^*} = \frac{1}{Ma} \frac{(1 + 0.2\ Ma^2)^3}{1.728} \quad .$$

Once the Mach number is known we solve for free stream temperature and pressure by

$$T_\infty = \frac{T_0}{1 + 0.2\ Ma^2} \quad ,$$

$$P_\infty = P_0\ (1 + 0.2\ Ma^2)^{-3.5} \quad .$$

Several values of free stream temperature and pressure are shown in Figure 7.

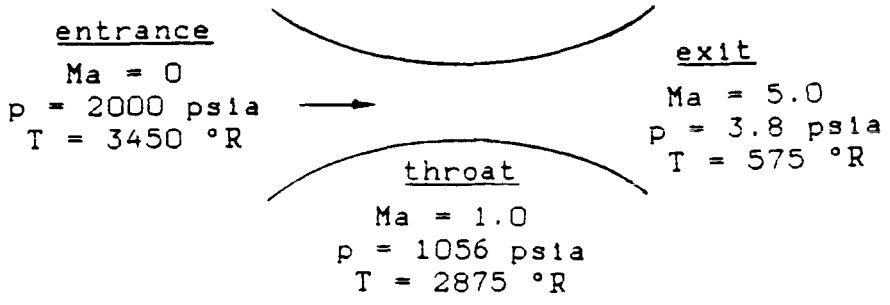

Figure 7. Compressible flow analysis.

Thermal Analysis

A cross section of the nozzle wall is given in Figure 8.

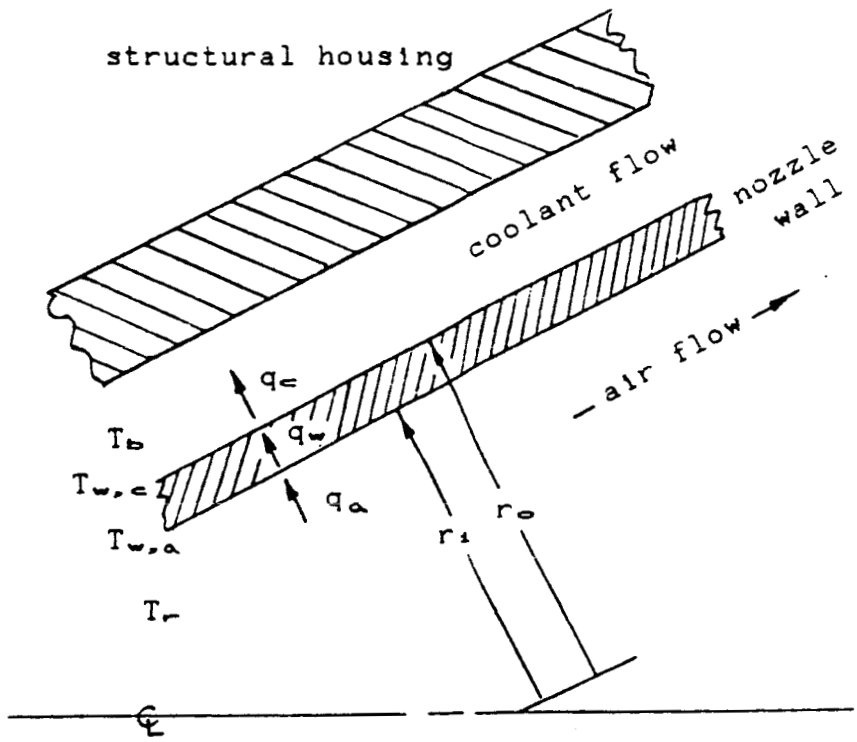

Figure 8. Heat transfer through the nozzle wall.

With reference to Figure 8 we can write

$$q_a = q_w = q_c \quad . \tag{1}$$

The assumptions are:

1. steady state conditions.
2. negligible conduction in the wall parallel to its surface.
3. negligible radiation from the air.

Using Newton's law of cooling for the first and last terms in Equation 1 and Fourier's law of conduction for the center term we have

$$q_a = A_a \, h_a \, (T_r - T_{w,a}) \quad , \tag{2}$$

$$q_c = A_c \, h_c \, (T_{w,c} - T_b) \quad , \tag{3}$$

$$q_w = -A_r \, k \, \frac{\partial T}{\partial r} \doteq \frac{2\pi \Delta L \, k \, (T_{w,a} - T_{w,c})}{\ln (r_o/r_i)} \quad . \tag{4}$$

The heat transfer on the air side comes from Bartz [1]. The complete development is given in Appendix B. Here we may write

$$h_a = (St \, c_p \, U \, \rho)_{air} \quad . \tag{5}$$

The heat transfer on the coolant side is from Rohsenow and Hartnett [2]. The complete development of this analysis appears in Appendix C. The result is

$$h_c = 0.0216\ (k/D_h)\ Re_{D_h}^{0.8}\ Pr^{1/3}\ (\mu/\mu_w)^{0.14} \quad . \qquad (6)$$

We can now obtain expressions for the wall temperature on the air and coolant sides ($T_{w,a}$, $T_{w,c}$) by manipulating Equations 1 through 6. The result is

$$T_{w,a} = \frac{T_r\ r_i\ h_a + \dfrac{k\ T_{w,c}}{\ln(r_o/r_i)}}{\dfrac{k}{\ln(r_o/r_i)} + r_i\ h_a} \quad , \qquad (7)$$

and

$$T_{w,c} = \frac{\dfrac{k\ \ T_{w,a}}{\ln(r_o/r_i)} + h_c\ r_o\ T_b}{r_o\ h_c + \dfrac{k}{\ln(r_o/r_i)}} \quad . \qquad (8)$$

We now find that

$$T_{w,a} = T_{w,a}\ (h_a\ ,\ T_{w,c}) \quad , \qquad (7)$$

$$h_a = h_a\ (T_{w,a}) \quad , \qquad (5)$$

$$T_{w,c} = T_{w,c}\ (T_{w,a}\ ,\ h_c) \quad , \qquad (8)$$

$$h_c = h_c\ (T_{w,c}) \quad . \qquad (6)$$

Because of the implicit nature of Equations 7, 5, 8 and 6 the solution is obtained by the numerical method of successive substitution. Details of the computer code which performs these operations are given in Appendix D.

Equations 7 and 8 give the temperature of the nozzle wall. For design considerations the maximum wall temperature $T_{w,max}$ must not exceed the corrosion temperature of the material. Therefore we define a Margin of Safety for Temperature

$$\text{Margin of Safety for Temperature} = T_{w,max} - T_{corrosion} \quad . \quad (9)$$

Stress Analysis

The thermal gradient and differential fluid pressure across the nozzle liner set up a state of stress. The principle of superposition allows us to calculate these stresses independently and then simply add them together. Thermal stress was calculated using the long hollow-cylinder equations assuming a logarithmic temperature distribution according to Timoshenko [3]. Justification for a logarithmic temperature distribution as a function of radial distance is given in Appendix E. Stresses will be greatest at either surface. At the inside radius the circumferential and axial components of thermal stress are given by

$$\sigma_{\theta,i} = \sigma_{z,i} = \frac{\alpha E \Delta T \left[1 - \frac{2 r_o^2 \ln(r_o/r_i)}{r_o^2 - r_i^2}\right]}{2 (1 - \nu) \ln(r_o/r_i)} \quad . \quad (10)$$

and the radial component of thermal stress is given by

$$\sigma_{r,i} = 0 \quad . \tag{11}$$

At the outside radius circumferential and axial components of thermal stress are given by

$$\sigma_{\theta,o} = \sigma_{z,o} = \frac{\alpha E \Delta T \left[1 - \frac{2 r_i^2 \ln(r_o/r_i)}{r_o^2 - r_i^2}\right]}{2 (1 - \lambda) \ln(r_o/r_i)} \quad , \tag{12}$$

and the radial component of thermal stress is given by

$$\sigma_{r,o} = 0 \quad . \tag{13}$$

The material properties appearing in Equations 10 and 12 are dependent on temperature. The pressure stresses are calculated using Timoshenko's thick-walled pressure vessel theory. It should be noted that thermal stresses are up to 18 times greater than pressure stresses in the critical areas near the throat (see Appendix F). For this reason the axial components of pressure stress, which are a complicated function of the nozzle geometry, are omitted. At the inside radius the circumferential component of pressure stress is given by

$$\sigma_{\theta,i} = \frac{P_\infty (r_o^2 + r_i^2)}{r_o^2 - r_i^2} - \frac{2 P_c r_o^2}{r_o^2 - r_i^2} \quad , \tag{14}$$

where P_∞ is the local air side pressure and P_C is the coolant pressure. The radial component of pressure stress is given by

$$\sigma_{r,i} = -P_\infty \quad . \tag{15}$$

At the outside radius the circumferential component of pressure stress is given by

$$\sigma_{\theta,o} = \frac{2 P_\infty r_i^2}{r_o^2 - r_i^2} - \frac{P_c (r_o^2 + r_i^2)}{r_o^2 - r_i^2} \quad , \tag{16}$$

and the radial component of pressure stress is given by

$$\sigma_{r,o} = -P_c \quad . \tag{17}$$

The theory of failure used here is described by Shigley and Mitchell [4]. It is called the distortion energy theory of failure. The triaxial stress state is calculated as

$$\sigma_y = \left\{ 1/2 \left[(\sigma_\theta - \sigma_r)^2 + (\sigma_\theta - \sigma_z)^2 + (\sigma_z + \sigma_r)^2 \right] \right\}^{1/2} \quad . \tag{18}$$

For design considerations the maximum triaxial state of stress must not exceed the yield strength of the material at the operating temperature. Therefore we define a Factor of Safety for Stress

$$\text{Factor of Safety for Stress} = \frac{S_y}{\sigma_{y,max}} \quad . \tag{19}$$

Before the blowdown process begins, the air side of the nozzle wall experiences a hard vacuum, while the coolant side is subjected to the full coolant pressure of 2000 psia. Failures that are possible during this pre-blowdown condition are discussed in Appendix G.

Material Analysis

The obvious criteria for material selection are Factor of Safety for Stress and Margin of Safety for Temperature. There are, however, two additional considerations. The first is wall thickness. Preliminary analyses have shown that a thin wall is necessary due to thermal stress. But from a practical point of view thin walls are difficult to fabricate, require delicate handling, and provide little allowance for loss of material due to corrosion and erosive "sandblasting" that occurs when the wind tunnel is operated.

The second additional consideration is that the wall temperature on the coolant side must not exceed the saturation temperature of the coolant. Tong [5] has described two phase boiling heat transfer and demonstrates that local nucleate boiling at the heat transfer surface (the coolant side wall in this case) actually increases heat transfer up to the "boiling crisis" temperature. Boiling crisis occurs when local boiling has advanced to the point that a bubble layer effectively insulates the heat transfer surface from

the coolant causing a radical increase in the surface temperature. This kind of temperature rise is undesirable and may lead to material failure. Using expressions from Tong, and with water as the coolant, we find that boiling crisis occurs approximately 35 °C above the saturation temperature for a large range of coolant pressures. Due to possible inaccuracies in the overall computer model temperature calculations for the current application, boiling is prohibited for this design. The upper limit for $T_{w,c}$ is therefore the critical point for water where the temperature and pressure are 374 °C (705 °F) and 22.1 MPA (3206 psia) respectively. Saturation temperatures corresponding to lower pressures are given in Table 1.

Table 1.

Saturation Temperatures and Pressures for Water

Pressure		Temperature	
MPa	psig	°C	°F
6.9	1000	285	545
10.3	1500	313	596
13.8	2000	335	636
17.2	2500	353	668
20.7	3000	368	695

Summarizing the criteria for material selection we have:

1. Factor of Safety for Stress.
2. Margin of Safety for Temperature.
3. Wall thickness.
4. Coolant side wall temperature.

Preliminary analysis indicates that thermal stress dominates over pressure stress and that the thermal stress on the air side is slightly greater than on the coolant side. The thermal stress on the air side of the nozzle liner was given in Equation 10 and is repeated here.

$$\sigma = \frac{\alpha E \Delta T \left[1 - \frac{2 r^2 \ln(r_o/r_i)}{r_o^2 - r_i^2}\right]}{2 (1 - \lambda) \ln(r_o/r_i)} \quad . \tag{20}$$

The ΔT is obtained from the heat transfer through the wall.

$$q = \frac{2 \pi k L (\Delta T)}{\ln(r_o/r_i)} \quad . \tag{21}$$

Solving for ΔT

$$\Delta T = \frac{q}{2 \pi k L} \ln(r_o/r_i) \quad .$$

Substituting Equation 21 into 20 gives

$$\sigma = \frac{\alpha E}{k} \left\{ \frac{q}{4 \pi L (1 - \lambda)} \left[1 - \frac{2 r_o^2 \ln(r_o/r_i)}{r_o^2 - r_i^2}\right]\right\} \quad . \tag{22}$$

For a nozzle liner of fixed wall thickness the term in the braces of Equation 22 is relatively constant. Although

q increases with an increase in k it is only weakly dependent. We therefore write

$$\sigma = \frac{\alpha E}{k} C_1 \quad ,$$

where C_1 is a constant. Recalling the Factor of Safety for Stress

$$F.S. = \frac{S}{\sigma} \quad .$$

So

$$F.S. = \frac{S}{\frac{\alpha E}{k} C_1} \quad ,$$

Or

$$F.S. \propto \frac{S\ k}{\alpha\ E} \quad . \tag{23}$$

We conclude from Equation 23 that in order to satisfy the Factor of Safety for Stress the material selected must have a relatively high yield strength and high thermal conductivity, and a relatively low coefficient of thermal expansion and low modulus of elasticity. Candidate materials that possess the above properties at elevated temperatures are given in Table 2.

Table 2.

Candidate Materials.

material	thermal conductivity Btu/ft hr °F	tensile strength ksi	modulus elasticity ksi	thermal expansion coefficient in/in °F	$\frac{S\ k}{\alpha\ E}$ Btu/ft hr
TZM	58	71	32.0 E3	3.0 E-6	42.9 E3
GLIDCOP AL-15	186	22-32	17.0 E3	9.2 E-6	32.7 E3
AMAX-MZC	150-200	27	18.2 E3	9.0 E-6	28.8 E3
AMZIRC	193	20	18.7 E3	10.8 E-6	19.1 E3
WC-103	22	40	13.4 E3	4.1 E-6	16.0 E3
BERYLCO	77	goes to zero at 1150 °F	18.5 E3	9.9 E-6	-

CHAPTER 4

Results and Discussion

The optimum design

Using the mathematical model developed in the analysis chapter we are now ready to select from the following design parameters: the material, wall thickness, coolant flow rate, coolant pressure and bulk temperature. This will produce a final design which gives the optimum combination of Factor of Safety for Stress and Margin of Safety for Temperature. Additional constraints are a practical wall thickness and the wall temperature on the coolant side lower than the coolant boiling temperature. Initial examination of the design parameters led to the range and combination of parameters given in Table 3.

The results of the analysis for the combinations of design parameters given in Table 3 appear in Figures 9 through 13. The selected design calls for TZM with minimum wall thickness of 2 millimeters, and coolant flow rate of 25 m/s at 300 K and 2000 psia. The three graphs in Figure 9 plot various quantities against the nozzle axial location for the design case. Figure 9a gives the results of the flow analysis; Figure 9b gives the results of the thermal analysis; and Figure 9c gives the results of the stress analysis.

Table 3.

Selection of Design Parameters.

material*	flow rate	wall thickness	coolant bulk temperature
TZM	10 m/s	2.0 mm	300 K
TZM	15	2.0	300
TZM	20	2.0	300
TZM	25	2.0	300
TZM	30	2.0	300
TZM	25	1.0	300
TZM	25	1.5	300
TZM	25	2.0	300
TZM	25	2.5	300
TZM	25	3.0	300
TZM	25	2.0	300
TZM	25	2.0	350
TZM	25	2.0	400
GLIDCOP	25	2.0	300
AMZIRC	25	2.0	300
WC-103	25	2.0	300

* TZM is molybdenum alloyed with titanium and zirconium.
GLIDCOP is copper alloyed with an aluminum oxide.
AMZIRC is copper alloyed with zirconium.
WC-103 is a columbium base alloy.

The axial locations span from 7 cm upstream of the throat to 2 cm downstream of the throat. The reason for terminating the information downstream of the 2 cm location is two fold: first, the temperatures and pressures are rapidly decreasing at this point and beyond since we are well past the critical location just upstream of the throat; second, the computations become time consuming due the numerical solution of h_a as described in Appendix C.

In Figure 9a the pressure, temperature and Mach number of the air throughout the nozzle are given. Figure 9b gives the heat transfer coefficient, heat flux and wall temperatures. Notice that all of these parameters peak at about 0.5 cm upstream of the throat. In Figure 9c the Factor of Safety for Stress and Margin of Safety for Temperature reach their relative minimums at this 0.5 cm upstream location.

The effect of varying the nozzle wall thickness can be seen in Figure 10. Coolant speed was held constant at 25 m/s. Coolant bulk temperature was held constant at 300 K. Recall from the analysis in Chapter 3 that boiling must not be permitted. For a wall thickness of 1.5 mm a coolant pressure greater than 2000 psi is needed. Furthermore, for reasons stated earlier, we would like to have the wall as thick as possible. For a wall thickness of 2.5 mm a coolant pressure of 1500 psi is sufficient, but notice that the air side wall temperature is close to the corrosion temperature. The wall thickness of 2.0 mm provides a Margin of Safety for

Temperature of 50 °C, and a Factor of Safety for Stress of about 1.4. A coolant pressure of 2000 psi is sufficient to prevent boiling. Based on the information in Figure 10 a nozzle liner thickness of 2.0 mm was selected.

Figure 11 shows the effect of varying the coolant speed. In this case the liner wall thickness was held constant at 2.0 mm, and the coolant bulk temperature was held constant at 300 K. Again, the boiling temperatures of water at various pressures are superimposed. A coolant speed of 20 m/s results in a coolant side wall temperature which cannot prevent boiling for water pressure at 2000 psia. A coolant speed of 30 m/s causes a significant reduction in coolant side wall temperature, but does not significantly affect the Factor of Safety for Stress. Figure 11 indicates that a coolant speed of 25 m/s and a coolant pressure of 2000 psia is optimum.

Figure 12 shows the effect of varying the coolant bulk temperature. In this case we see that the bulk temperature over a range of 300 to 400 Kelvin has little effect on the wall temperatures or the Factor of Safety for Stress.

Figure 13 shows the effect of using materials other than TZM. From this figure we see that TZM is the only material with Factor of Safety greater than 1.0 for liner thickness of 2 mm, coolant bulk temperature of 300 K, and coolant speed of 25 m/s. There is a possibility that some other set of conditions might result in greater Factors of

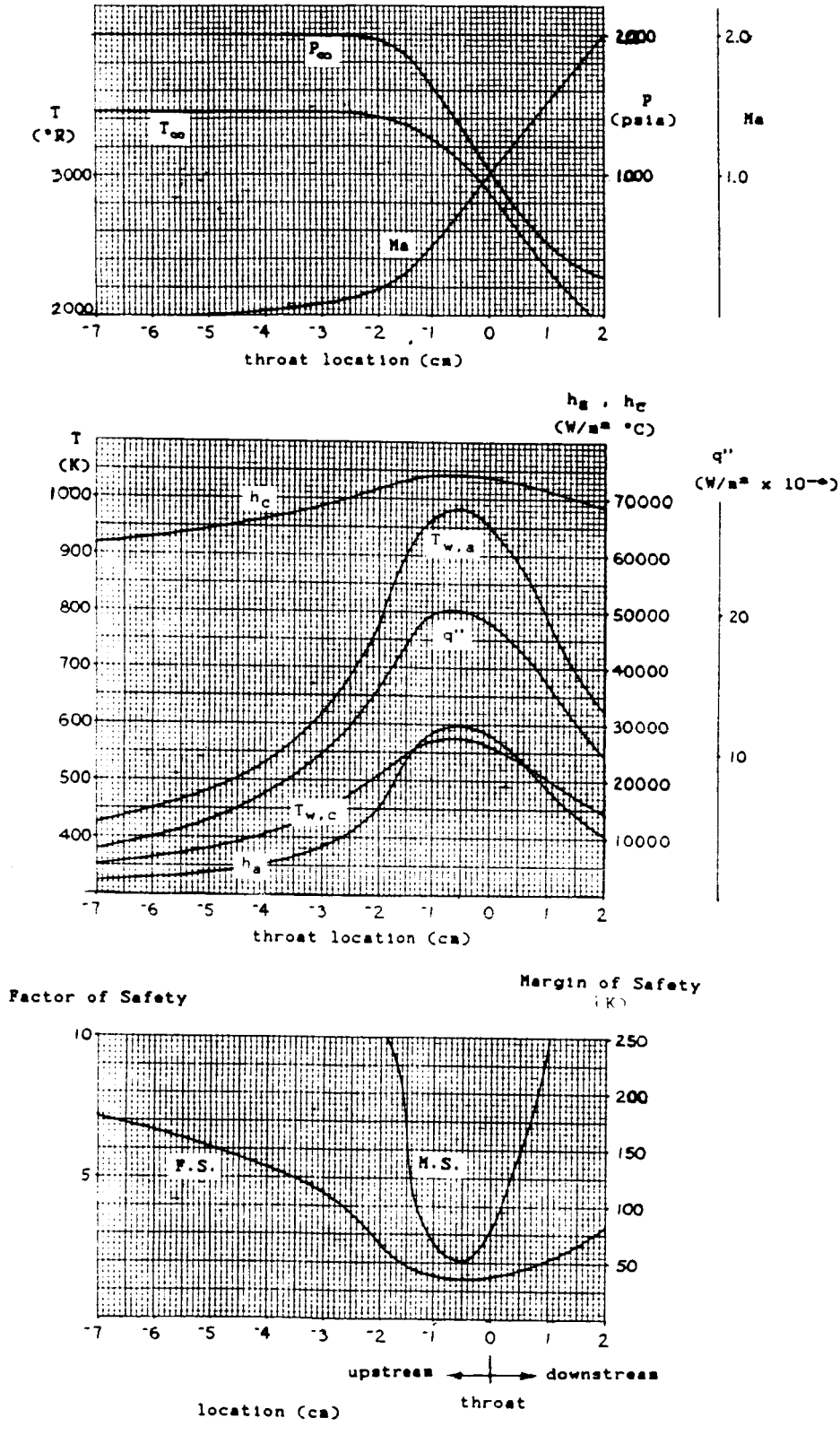

Figure 9. Results of the flow, thermal and stress analyses for a nozzle of TZM material with 2.0 mm wall thickness, 25 m/s coolant flow, 2000 psia coolant pressure and 300 K coolant temperature.

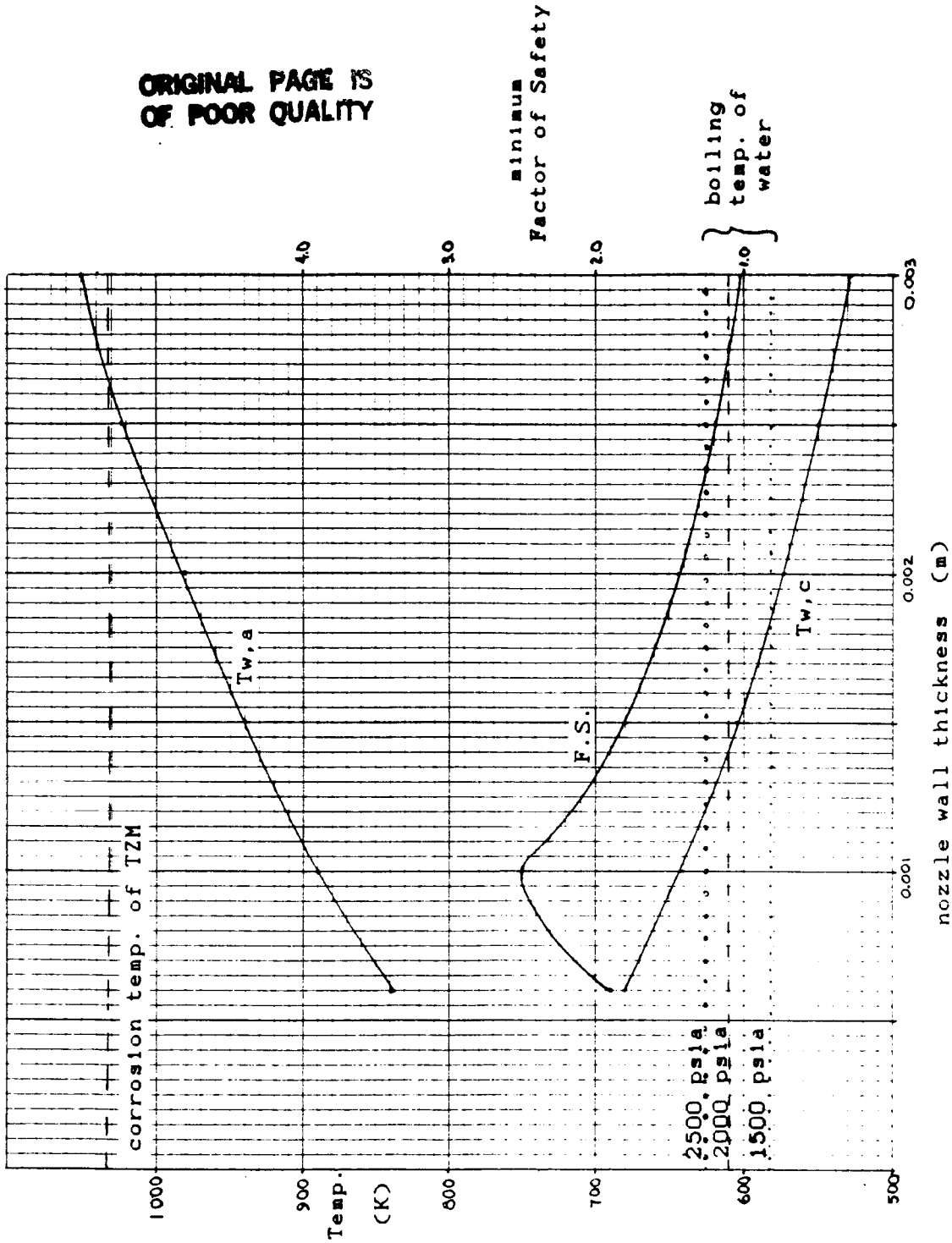

Figure 10. The effect of nozzle wall thickness. Material is TZM with coolant flow rate 25 m/s and coolant temperature 300 K.

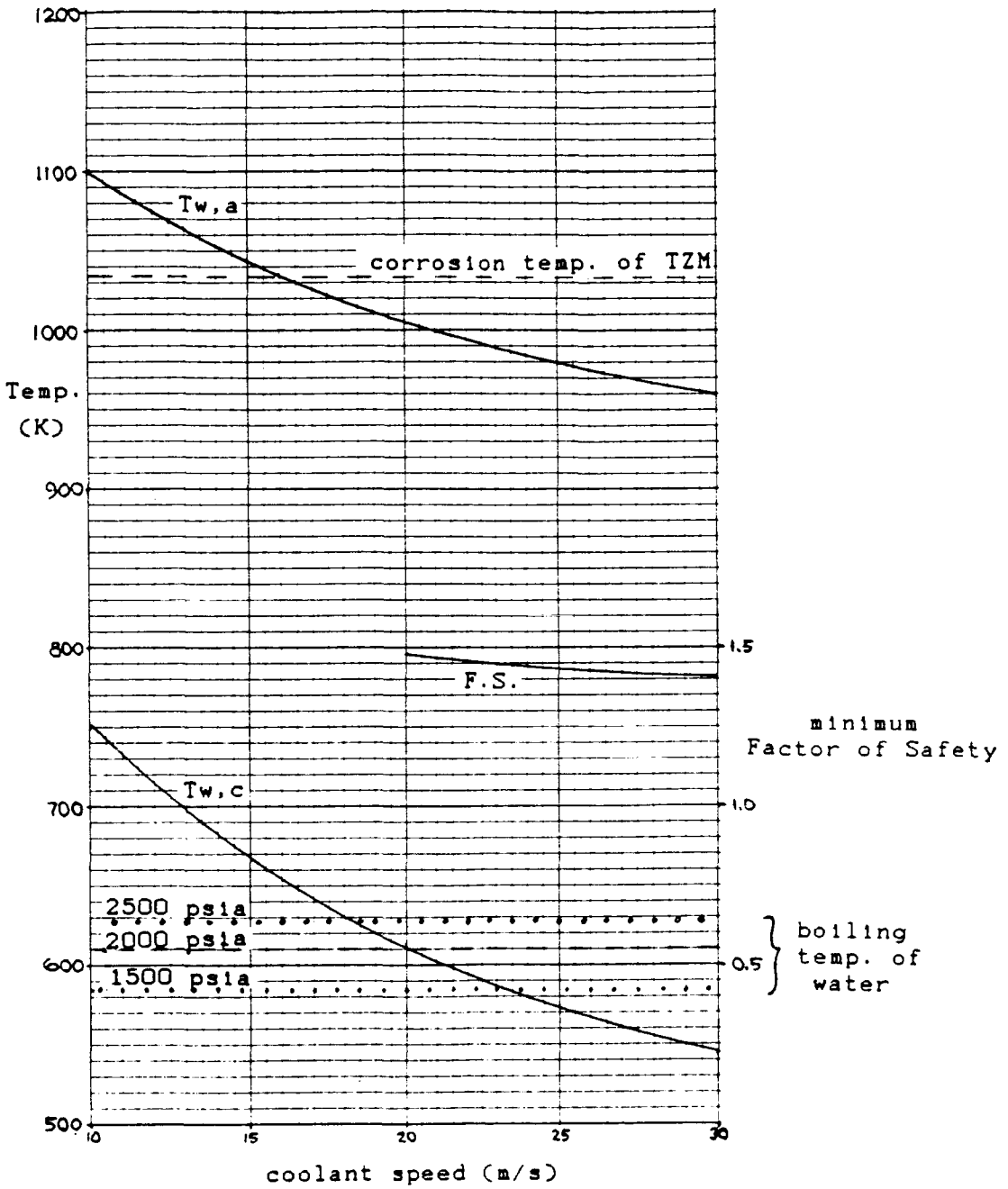

Figure 11. The effect of coolant speed. Material is TZM with wall thickness 2.0 mm and coolant temperature 300 K.

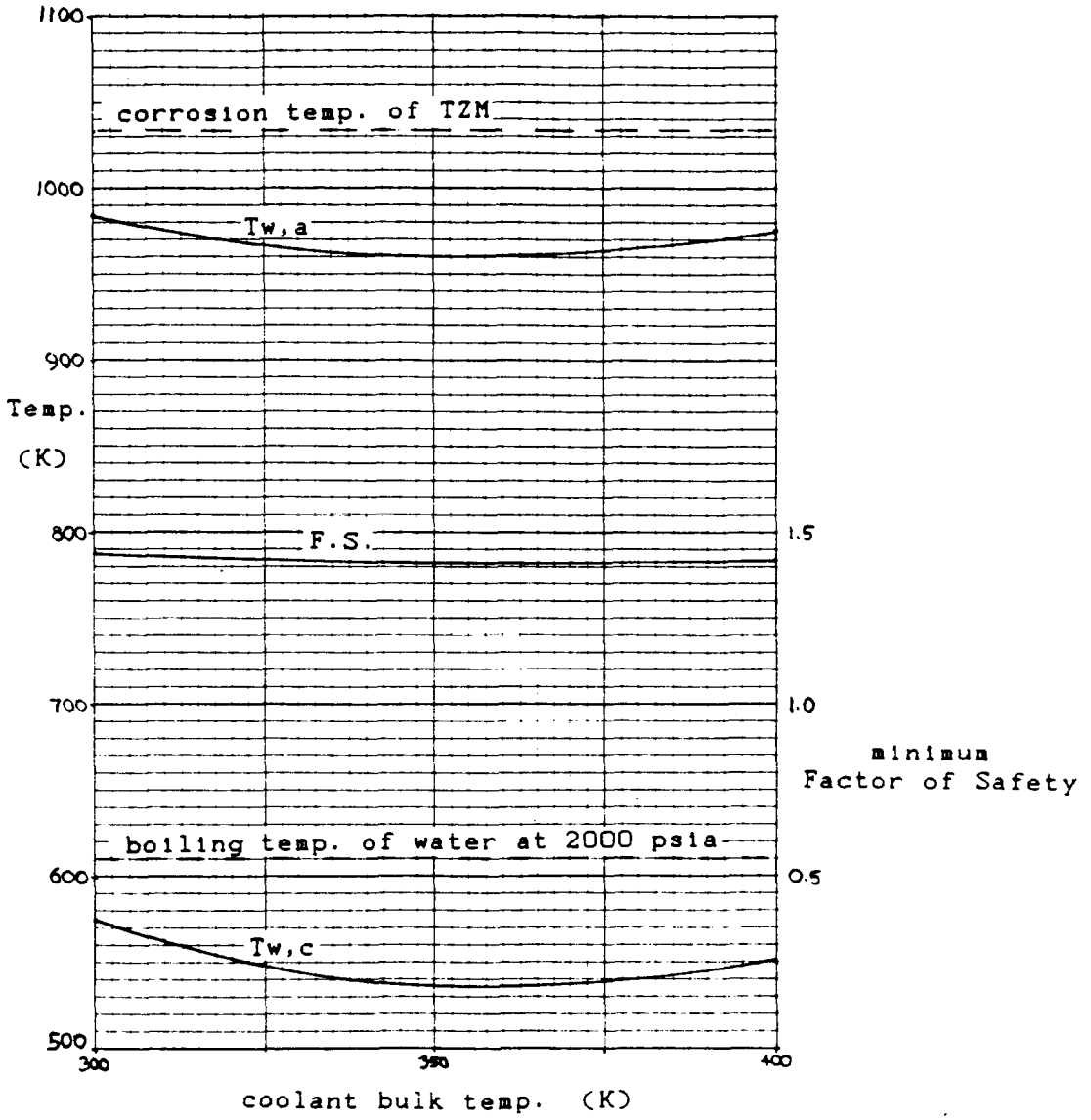

Figure 12. The effect of coolant bulk temperature. Material is TZM with wall thickness 2.0 mm and coolant flow rate 25 m/s.

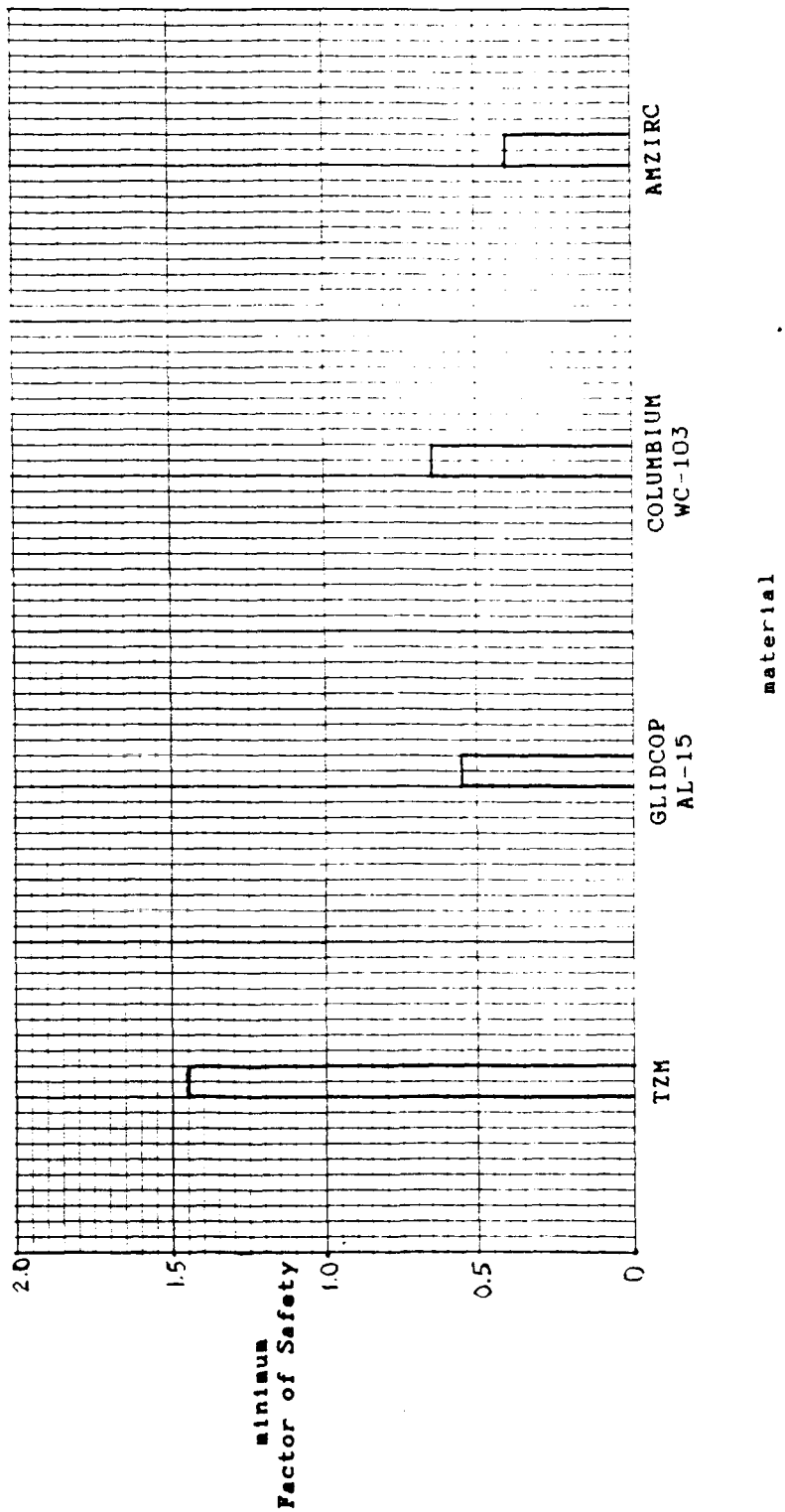

Figure 13. The effect of various materials.

Safety for the other materials. However, experience has shown that the molybdenum alloy TZM always outperforms the other candidate materials.

Start-up Considerations

Next we consider start-up conditions. We define start-up conditions as wind tunnel operating conditions below the design 2000 psia pressure and 3460 °R temperature. The results of this analysis will predict the nozzle wall temperature over a range of start-up conditions. These predictions can be compared with temperature measurements made during start-up operation. If measured temperatures match predicted temperatures, we then can be confident that the nozzle will perform well at 3460 °R and 2000 psia.

Analysis of the final nozzle design were performed at the start-up temperatures and pressures shown in Table 4. The result of this work appears in Figures 14, 15, 16 and 17. In Figures 14, 15 and 16 the coolant wall temperatures are presented over the length of the nozzle for inlet air pressures of 1000, 1500, 2000 psia and inlet air temperatures of 2300 °R, 3200 °R and 3460 °R. Temperature measurements may be made with a thermocouple located away from the critical area near the throat. Such a location would be 2 cm downstream of the throat. Figure 17 predicts the coolant side wall temperature at 2.0 cm downstream of

the throat during steady state operation at inlet air pressures of 1000, 1500, and 2000 psia, and over a range of inlet air temperatures from 2300 °R to 3460 °R.

Table 4.

Start-up Temperatures and Pressures.

Inlet Air Temperature	Inlet Air Pressure
2300 °R	1000 psia
2300	1500
2300	2000
3200	1000
3200	1500
3200	2000
3460	1000
3460	1500

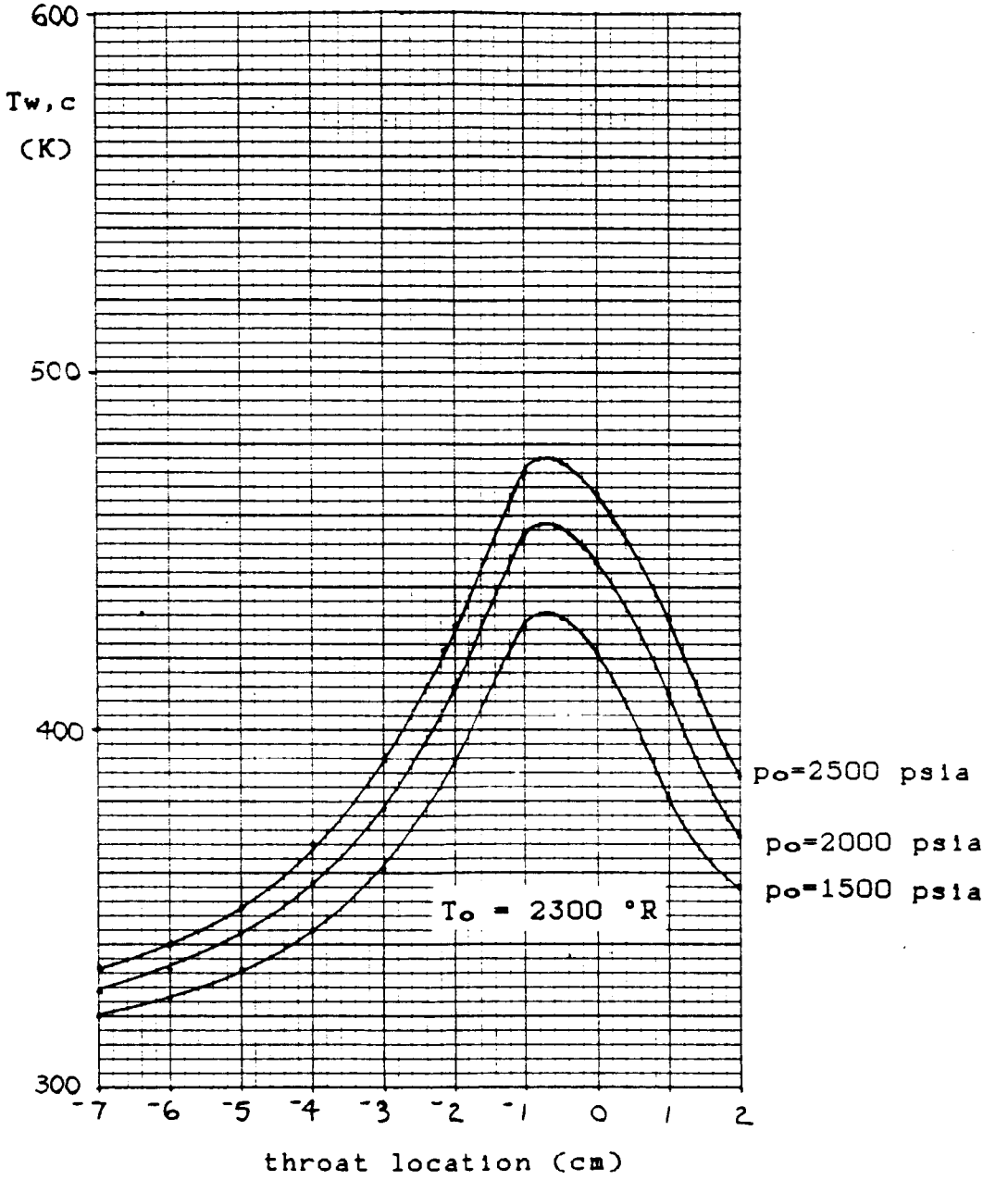

Figure 14. Nozzle temperatures during start-up conditions.

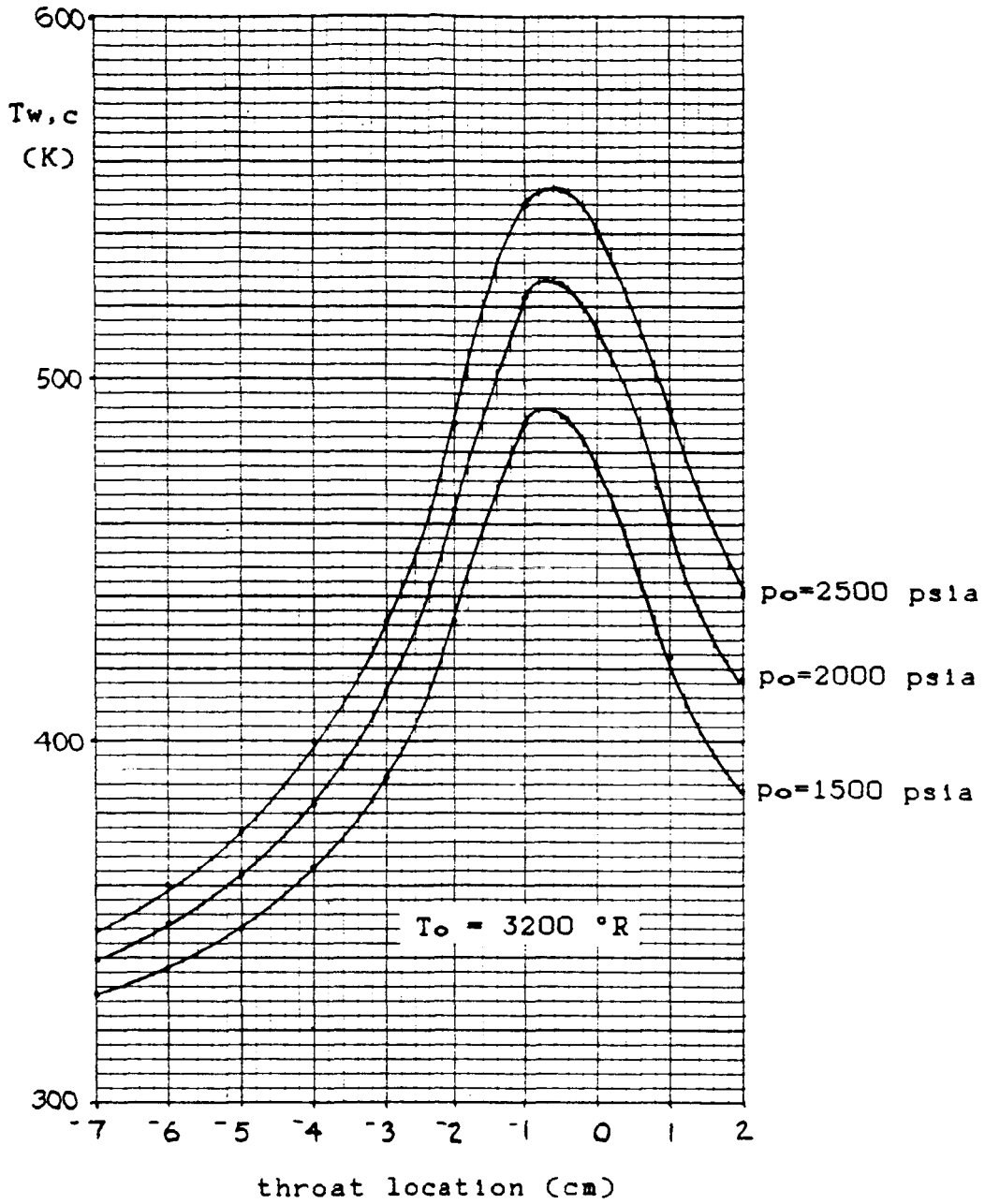

Figure 15. Nozzle temperatures during start-up conditions.

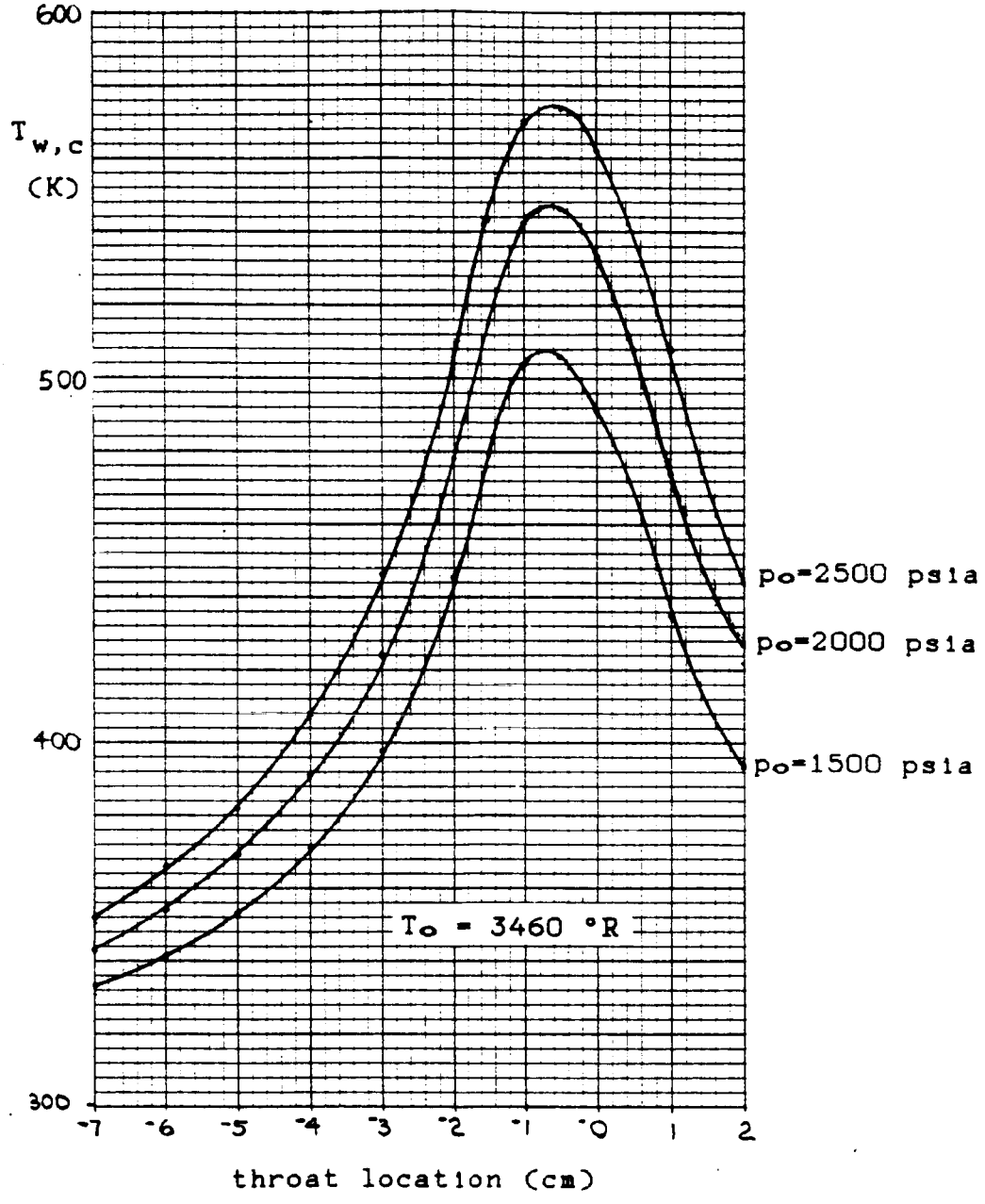

Figure 16. Nozzle temperatures during start-up conditions.

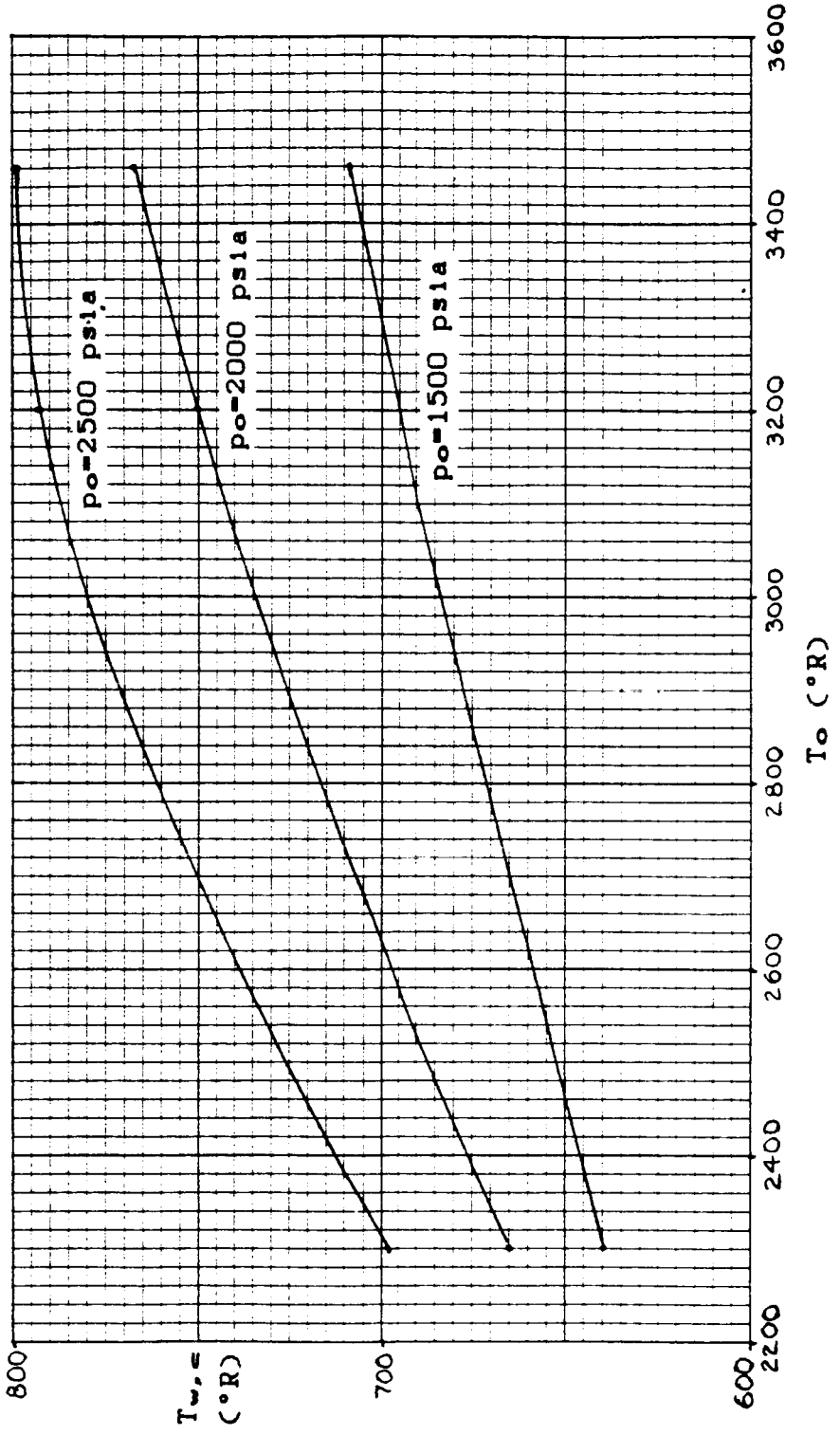

Figure 17. Nozzle temperatures during start-up conditions at the location 2.0 cm downstream of the throat.

CHAPTER 5

Conclusions and Recommendations

The results of the analysis support the following conclusions with regard to the nozzle shown in Figure 6:

1. The material should be TZM as specified in the Metals Handbook [9]. This material can be obtained from AMAX Specialty Metals Corp. [6]. Viking Metallurgical [7] or Northwest Industries [8] appear capable of fabricating the design.

2. The wall thickness should be 2.0 mm along the length of the wall adjacent to the coolant passage surrounding the throat area. The wall then tapers to 4.0 mm thick at the downstream flange, and 4.0 mm thick at the upstream end.

3. The coolant should be water pressurized to 2000 psi, with a bulk temperature around 300 K and flowing at 25 m/s in the coolant passages. This corresponds to a flow rate of 127 gal/min.

We recommend the installation of a thermocouple 2.0 cm downstream of the throat on the coolant side of the nozzle wall. Temperature measurements from the thermocouple may be compared with temperatures predicted from the analysis providing a means of validating the analysis.

REFERENCES

1. Bartz, D.R., in Advances in Heat Transfer (Hartnett, J.P., ed.),Academic Press, New York, 1965

2. Rohsenow, W.M., and J.P. Hartnett, Handbook of Heat Transfer, Mcgraw-Hill Book Company, New York, 1973.

3. Timoshenko, S.P., and J.N. Goodier, Theory of Elasticity, 3rd ed., McGraw-Hill Book Company, New York, 1970.

4. Shigley, J.E., and L.D. Mitchell, Mechanical Engineering Design, 4th ed., McGraw-Hill Book Company, New York, 1983.

5. Tong, L.S., Boiling Heat Transfer and Two-Phase Flow, John Wiley & Sons, Inc., New York, 1965.

6. AMAX Specialty Metals Corp.
   23232 Peralta, Suite 119
   Laguna Hills, CA 92653

7. Quanex Viking Metallurgical
   No. 1 Erik Circle
   Verdi, NV 89439-0339

8. Northwest Industries Inc.
   P.O. Box 550
   Albany, OR 97321

9. ASM Review Board, Metals Handbook, American Society for Metals, Metals Park, OH, 1979.

10. Kern, D.Q., and A.D. Kraus, Extended Surface Heat Transfer, McGraw-Hill Book Company, New York, 1972.

11. Jahnke, E., G. Emde, and F. Losch, Tables of Higher Functions, McGraw-Hill Book Company, New York, 1960.

12. Bartz, D.R., "A simple equation for rapid estimation of rocket nozzle convective heat transfer coefficients." Jet Propulsion, 27, 49-51, 1957.

13. Sieder, E.N., and G.E. Tate, Ind. Eng. Chem., 28, 1429, 1936.

14. Incropera, F.D., and D.P. Dewitt, Introduction to Heat Transfer, Wiley, New York, 1985.

15. Gambill, W.R., and R.D. Bundy, Nuc. Sci. Engr., 18, p.69, 1964.

16. Kays, W.M., and M. E. Crawford, Convective Heat and Mass Transfer, McGraw-Hill Book Company, New York, 1980.

17. Kays, W.M., Trans. ASME, 77, p.1265, 1955.

18. Hausen, H.Z. VDI. Beih. Verfahrenstech, 4, p.91, 1943.

19. Whitaker, S., AICHE J., 18, p.361, 1972.

20. Shah, R.K., and A.L. London, Laminar Flow Forced Convection in Ducts, Academic Press, New York, 1978.

21. Reynolds, W.C., Int. J. Heat Mass Transfer, 6, p.925, 1963.

22. Sparrow, E.M. and S.H. Lin, Int. J. Heat Mass Transfer, 6, p. 800, 1963.

23. Ito, H., "Friction factors for turbulent flow in curved pipes." J. Basic Engr., 123-134, June, 1959.

24. Kreith, F., Heat Transfer in Curved Flow Channels, Heat Transfer Fluid Mechanics Institute, pp. 111-122, ASME, 1953.

25. Yang, J.W. and N. Liao, Turbulent Heat Transfer in Rectangular Ducts with 180° Bend, Proceedings of the Fifth International Heat Transfer Conference. Sept., 1974, Tokyo, Japan Society of Mech. Engr.

26. Faupel, J.H., Engineering Design, John Wiley and Sons, Inc., New York, 1964.

APPENDIX A

Optimization of fin geometry

The differential equation describing steady state heat transfer in a radial fin with rectangular profile is given by Kern and Kraus [9] as:

$$r^2 \frac{d^2\theta}{dr^2} + r \frac{d\theta}{dr} - \frac{2h}{k \delta_o} r^2 \theta = 0 \quad , \qquad (A1)$$

where θ is ΔT, and δ_o is the fin thickness as shown in Figure A1. We let $m=(2h / k \delta_0)^2$, and note that Equation A1 is Bessel's modified differential equation with general solution:

$$\theta = C_1 I_0(mr) + C_2 K_0(mr) \quad . \qquad (A2)$$

Substituting boundary conditions

$$r = r_o \quad , \quad \theta = \theta_0 \quad , \qquad (A3a)$$

$$r = r_e \quad , \quad \frac{d\theta}{dr} = 0 \quad . \qquad (A3b)$$

into Equation A2 leads to

$$\theta_0 = C_1 I_0(mr_o) + C_2 K_0(mr_o) \quad , \qquad (A4a)$$

$$0 = C_1 I_1(mr_e) + C_2 K_1(mr_e) \quad . \qquad (A4b)$$

This leads to

$$\theta = \frac{\theta_0 \left[K_1(mr_e)\ I_0(mr) + I_1(mr_e)\ K_0(mr)\right]}{I_0(mr_o)\ K_1(mr_e) + I_1(mr_e)\ K_0(mr_o)} \quad . \qquad (A5)$$

Using Fourier's law of heat conduction at the base of the fin we have

$$q = -2\pi k r_o \delta_o \left.\frac{d\theta}{dr}\right|_{r=r_o} \quad . \tag{A6}$$

Differentiating Equation A5 at $r=r_o$ and substituting into Equation A6 we have

$$q_{\text{with fin}} = 2\pi k r_o \delta_o m \theta_o \left[\frac{I_1(mr_e) K_1(mr_o) - K_1(mr_e) I_1(mr_o)}{I_0(mr_o) K_1(mr_e) + I_1(mr_e) K_0(mr_o)}\right] \quad . \tag{A7}$$

We now calculate the heat transfer that would result if there were no fin:

$$q_{\text{without fin}} = 2\pi \delta_o r_o h \theta_o \quad . \tag{A8}$$

Comparing the heat transfer obtained with and without the fin:

$$\frac{q_{w/o\ fin}}{q_{w/\ fin}} = \frac{2\pi r_o \delta_o \theta_o h}{2\pi k r_o \delta_o m \theta_o} \left[\frac{I_1(mr_e) K_1(mr_o) - K_1(mr_e) I_1(mr_o)}{I_0(mr_o) K_1(mr_e) + I_1(mr_e) K_0(mr_o)}\right]^{-1} \quad .$$

but $m = (2h / k\delta_o)^2$. After cancellation:

$$\frac{q_{w/o\ fin}}{q_{w/\ fin}} = \left[\frac{h \delta_o}{2 k}\right]^{\frac{1}{2}} \left[\frac{I_1(mr_e) K_1(mr_o) - K_1(mr_e) I_1(mr_o)}{I_0(mr_o) K_1(mr_e) + I_1(mr_e) K_0(mr_o)}\right]^{-1} \quad . \tag{A9}$$

The term in brackets consists of four Bessel function coefficients, which are transcendental functions. They depend on m and the size of the fin. For the magnitudes encountered in the present study the term in brackets varies from 0.7 to 0.9. We will assign the conservative value of 0.7 to this term. Clearly, we want the ratio of heat transfer shown on the left hand side of Equation A9 to be less than one. However, in order to arrive at a general guideline in the optimization process we will temporarily set Equation A9 equal to unity. Then, carrying out the algebra and solving for the Biot number:

$$Bi = (h\ \delta_o)/k \approx 1.0 \quad .$$

Thus, in order to justify the use of fins, this ratio would need to be significantly less than 1.0. Note that as the Biot number decreases, cooling fins become more and more justifiable.

Substituting typical values from our study for the variables we have

θ_o = 222 Kelvin

δ_o = 0.002 meters

r_o = 0.00769 meters

r_e = 0.0102 meters

h = 100,000 $W/m^2 \cdot K$

k = 100 $W/m \cdot K$

From Jahnke, Emde and Lösch [10] we have

$$I_0(mr_o) = I_0(7.7) = 323.1$$

$$I_1(mr_o) = I_1(7.7) = 301.1$$

$$I_1(mr_e) = I_1(10) = 2671$$

$$K_0(mr_o) = K_0(7.7) = 20142$$

$$K_1(mr_o) = K_1(7.7) = 21412$$

$$K_1(mr_e) = K_1(10) = 18648$$

Substituting these values into Equation A9 we have:

$$(h\ \delta_o)/k = 1.16 \quad . \tag{A10}$$

This ratio indicates that the presence of a fin actually <u>decreases</u> the amount of heat transfer. Due to the high convection coefficient on the coolant side as compared to the thermal conductivity and thickness of the fins we conclude that in this case cooling fins cannot improve heat transfer.

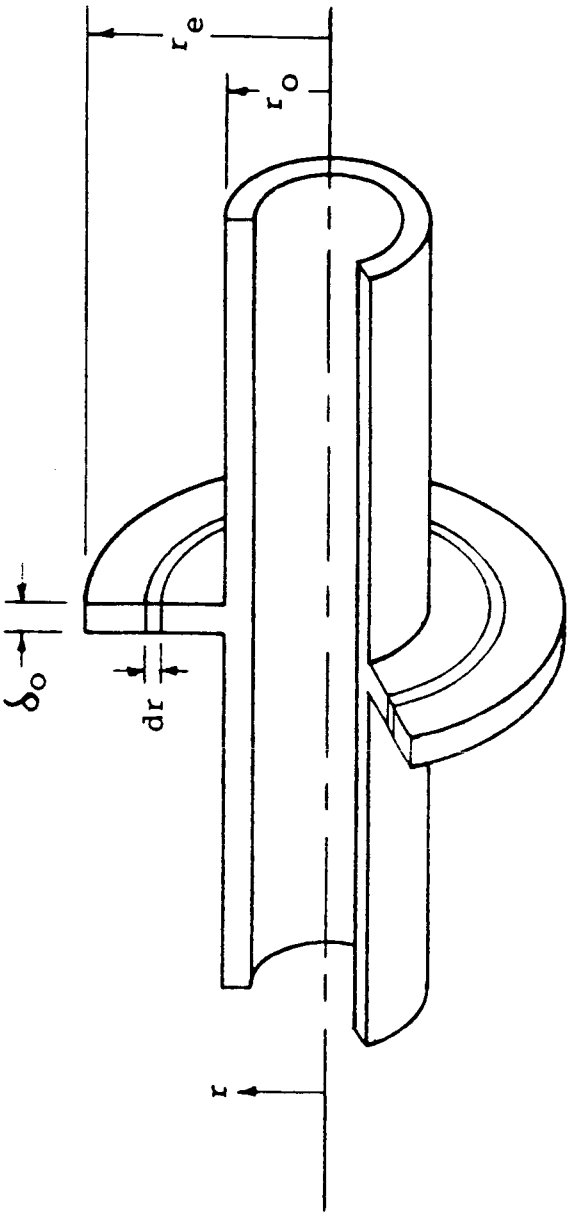

Figure A1. Radial fin with rectangular profile.

APPENDIX B

Air Side Heat Transfer

In a hypersonic wind tunnel acceleration of the gas (in this case dry air) is so great that simplifying assumptions usually made for duct flow no longer apply. Bartz [1] points out that the axial pressure gradient terms in the momentum and energy equations must be accounted for.

Using the integral momentum and energy equations we can solve for the Stanton number, St, as a function of axial location. The air side heat transfer coefficient as a function of axial location will then be given by

$$h_a = (St\ c_p\ U\ \rho)_{air} \quad , \tag{B1}$$

where U is the local free stream speed of the air, and and c_p are properties of air evaluated at the local free stream conditions. Bartz developed the equations necessary to solve for the local air side heat transfer coefficient. The assumptions made for this development are reproduced here in their entirety.

1. The flow is axisymmetric and steady without tangential components of velocity.
2. The boundary layer is confined to a distance from the wall which is small compared with the distance from the axis of symmetry.

3. The only forces acting on the gas are those due to pressure gradients and to skin friction at the wall.

4. The only changes in total enthalpy in the flow direction are those due to heat flux through the wall.

5. The flow immediately outside the boundary layer is reversible and adiabatic and parallel to the wall.

6. Static pressure is constant through the boundary layer perpendicular to the wall.

7. The gas is perfect; however, the restriction that specific heats be constant can be removed in computing the driving potential for heat flux.

8. The gas has a constant Prandtl number, a viscosity which varies as a power of the temperature, and a constant adiabatic recovery factor.

9. The skin-friction coefficient is the same as for constant-pressure constant-wall-temperature flow on a flat plate at the same free-stream conditions, wall temperature, and momentum thickness.

10. The Stanton number is the same as for constant-pressure constant-wall-temperature flow on a flat plate at the same free-stream conditions, wall temperature, and momentum thickness.

11. The Stanton number for unequal momentum and energy thicknesses is that for equal thicknesses multiplied by $(\phi/\theta)^n$, where n is a small "interaction exponent".

12. Heat transfer affects the skin-friction coefficient in either one of two ways: (a) there is no effect, and C_f is the same as for adiabatic flow, or (b) C_f is the same as for adiabatic incompressible flow at a density and viscosity evaluated at the arithmetic mean between the actual wall temperature and the free-stream static temperature.

13. The Stanton number for equal momentum and energy thicknesses is related to the skin-friction coefficient by von Karman's form of Reynolds' analogy.

14. Any chemical reactions in the boundary layer affect only the driving potential for heat flux.

15. The boundary-layer shape parameters θ/δ , Δ/δ , and δ^*/θ are those of 1/7 power profiles of velocity and of the difference between stagnation and wall temperature. Such profiles are typical of turbulent boundary layers on flat plates.

16. Heat transfer by thermal radiation is negligible compared with convection.

17. There is no significant net mass transfer from wall to gas or gas to wall.

The applicable equations that result from Bartz's work involve the axial gradients of the momentum and energy thicknesses:

$$\frac{d\theta}{dz} = \frac{C_f}{2}\left[1 + \left(\frac{dr}{dz}\right)^2\right]^{1/2} - \theta\left[\frac{2 - Ma^2 + (\delta^*/\theta)}{Ma\left(1 + \frac{\gamma - 1}{2} Ma^2\right)} \frac{dMa}{dz} + \frac{1}{r}\frac{dr}{dz}\right], \quad (B2)$$

and

$$\frac{d\phi}{dz} = St\left(\frac{T_r - T_{w,a}}{T_0 - T_{w,a}}\right)\left[1 + \left(\frac{dr}{dz}\right)^2\right]^{1/2} - \phi\left[\frac{1 - Ma^2}{Ma\left(1 + \frac{\gamma - 1}{2} Ma^2\right)} \frac{dMa}{dz} + \frac{1}{r}\frac{dr}{dz} - \frac{1}{T_0 - T_{w,a}} \frac{dT_{w,a}}{dz}\right], \quad (B3)$$

where

$$C_f = \frac{0.0256}{Re_\theta^{1/4}}\left[1/2\left(\frac{T_{w,a}}{T_\infty} + 1\right)\right]^{-0.6}, \quad (B4)$$

and

$$St = \frac{C_f/2\,(\phi/\theta)^{-0.1}}{1 - 5\,(C_f/2)^{0.5}\left[1 - Pr + \ln\left(\frac{6}{5\,Pr + 1}\right)\right]}. \quad (B5)$$

With initial values for θ and ϕ we can set up a finite difference numerical scheme for the solution of Equations B1 through B5 as a function of axial location. Bartz showed that values for θ and ϕ at the throat are quite independent of the initial values.

It should be noted that both Equations B2 and B3 contain the axial gradient of Mach number. This gradient is relatively small in the upstream section and the axial step size is allowed to be correspondingly large (0.25 cm in this case). However, just downstream of the throat this gradient becomes quite large and a much smaller step size is required (0.125 mm). The smaller step size means more time is

required for solution. Perhaps more importantly the possibility for cumulative round-off error increases.

Two other methods for calculation of the air side heat transfer coefficient were considered. The first was a simplified equation from Bartz [12] meant to be used for quick estimates of h_a. However, the results were shown to be always higher than Bartz's more involved solution (see reference [1]). Due to the critical nature of conditions at the throat, it was felt that an artificially high h_a would impose unnecessary restrictions on the design. For example, an extremely high h_a might force the design to have a very thin liner wall thickness at the throat, perhaps around one millimeter. Such a thin wall might compromise the design in terms of handling during installation, or erosive "sand-blasting" during operation. The simple calculation for h_a was rejected in favor of a more accurate model.

The second alternative method for calculation of the air side heat transfer coefficient was given in Rohsenow and Hartnett [2]. Here, a number of empirical formulas were used. This method yielded an h_a within about 30% of the other methods, although it was consistently low. Again, the accuracy of the results might be questioned in terms of the formula's applicability to hypersonic flow.

APPENDIX C

Coolant Side Heat Transfer

The cooling system configuration shown in Figure 6 of the main text consists of three coolant passages. Each passage is supplied by coolant transitioning from a circular tube to a rectangular passage. From the rectangular passage the flow is split and diverted over and around the nozzle liner as two curved rectangular ducts. This is shown in Figure C1.

Our objective is to predict, using published literature, the heat transfer from the nozzle liner to the coolant in the curved rectangular passageways. A problem exists, however, in that the literature does not directly give heat transfer information for our particular application. Instead, the heat transfer must deduced based on information available for other similar flow passage configurations and flow conditions.

Our cooling system falls under the classification of internal duct flow. As a start, for flows that are characterized by large property variations, the following equation is recommended by Sieder and Tate [13]

$$Nu_D = 0.027\ Re_D^{4/5}\ Pr^{1/3}\ (\mu/\mu_w)^{0.14} \quad , \qquad (C1)$$

with the following restrictions:

circular duct flow

turbulent flow

fully developed flow

smooth wall

uniform circumferential heat flux

$0.7 < Pr < 16{,}700$

$Re_D > 10{,}000$

$L/D > 10$

fluid properties at coolant bulk temperature (except μ_w)

Our flow passage and flow conditions do not conform to the restrictions imposed by Equation C1. The deviations are

1. rectangular cross section duct
2. flow is not fully developed
3. circumferential heat flux variation
4. curved flow passage

Each one of the above deviations are now discussed with the corresponding effect on Equation C1.

1. Rectangular cross section duct. Incropera and De Witt [14] report that Equation C1 may be used for noncircular ducts if the hydraulic diameter is used in the Nusselt and Reynolds numbers. The hydraulic diameter is defined as

$$D_h = 4A_c/P \quad . \tag{C2}$$

This substitution is confirmed by Gambill and Bundy [15] as reported in Rohsenow and Hartnett [2], where Equation C1 fit the data very well for water in a rounded corner rectangular channel.

2. Flow is not fully developed. The flow is definitely developing thermally (start of the thermal boundary layer) at the point where it splits to travel around the nozzle liner. Also, at this point there is some argument that it may be hydrodynamically developing (start of the velocity boundary layer) as well. For the combined thermal and hydrodynamic entry length situation considerable data are available for circular tubes [16,17,18,19,20], all of which can be summarized by

$$Nu_{D\ \text{entrance region}} > Nu_{D\ \text{fully developed region}} \quad . \tag{C3}$$

Since our configuration is not tube flow and clearly not a well defined entrance region we will not attempt to account for this effect. Any error associated with this omission is on the conservative side. That is, the heat transfer coefficient will be lower as a result of not accounting for developing flow.

3. Circumferential heat flux variations. The coolant passage is bounded on the top by the structural housing and on

the bottom by the nozzle liner as shown in Figure C2. The nozzle liner is heated, while the structural housing is not. This results in what is called a "circumferential heat flux variation". Rohsenow [2] reports the work of Reynolds [21], and Sparrow and Lin [22] that applies to circular tubes with fully developed flow under circumferential heat flux variations. We will not attempt to account for this effect due to differences in our flow and flow channel geometry from those reported. Again, any error associated with this omission is on the conservative side. The thermal boundary layer is building up on only one side of the channel. This has the effect of a longer thermal entrance region with associated higher heat transfer rates.

4. Curved flow passage. A number of investigations [23, 24,25] examined heat transfer and pressure drop in curved passages. From these papers a general conclusion can be drawn that heat transfer is greater on the concave side of the flow passage compared to the convex side. This is unfortunate since we want to cool the convex side only in our flow passage. Kreith [24] reports the results of his experimental work with water at $Re_D = 5 \times 10^4$ in a curved parallel plate channel with $r_i/r_o = 0.8$. This Reynolds number is close to our design Reynolds number. Additionally, our design radius ratio is $r_i/r_o = 0.7$. Kreith gives $Nu_{concave}/Nu_{convex}$ as a function of Prandtl number. Our T_b

will range from 300 K to 350 K, which corresponds to Prandtl number and $Nu_{concave}/Nu_{convex}$ as shown in Table C1.

Table C1.

Heat Transfer in a Curved Parallel Plate Passage.

T_b	Pr	$\frac{Nu_{concave}}{Nu_{convex}}$
300	5.85	1.55
350	2.33	1.49

In Table 1 we will take an average Nusselt number ratio of 1.5. From Yang and Liao [25], who performed experiments in rectangular ducts with 180 bend, we obtain the general relationship

$$(Nu_{concave} - Nu_{straight}) = (Nu_{straight} - Nu_{convex}) \qquad (C4)$$

Recalling that $Nu_{concave}/Nu_{convex} = 1.5$ gives

$$Nu_{convex} = 0.8\ Nu_{straight}. \qquad (C5)$$

$Nu_{straight}$ is the same as the Nu_D in Equation 1. Therefore Equation 1 is substituted into Equation 5 to give the final result for heat transfer on the coolant side

$$h_c = k/D_h\ 0.0216\ Re^{0.8}\ Pr^{1/3}\ (\mu / \mu_w)^{0.14} \qquad (C6)$$

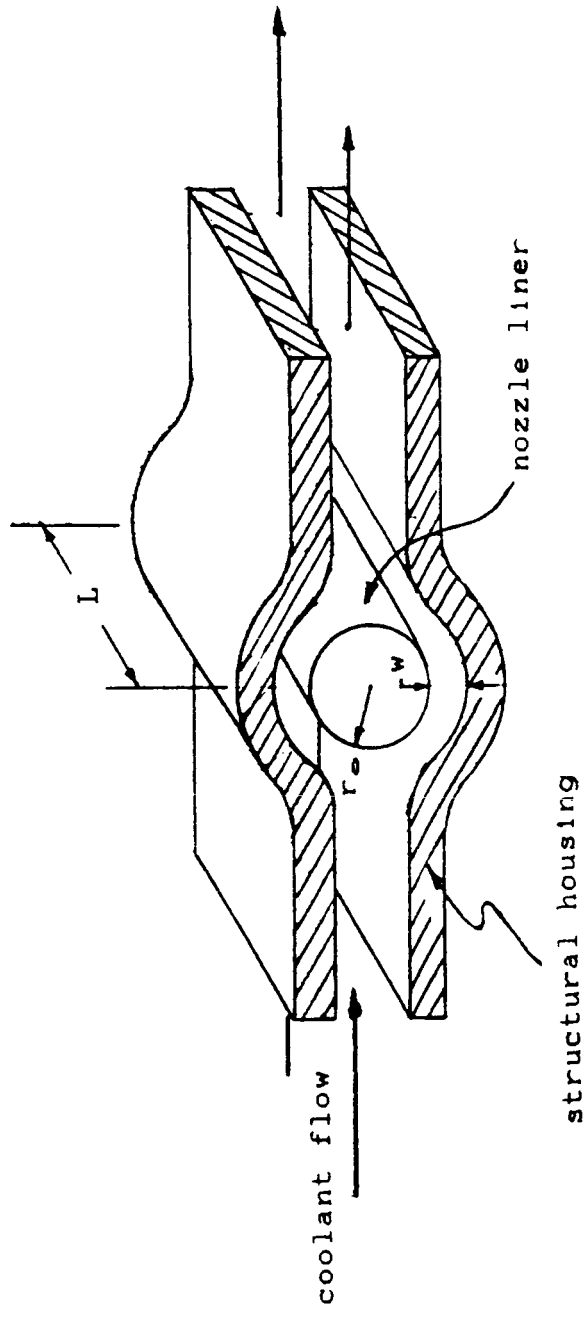

Figure C1. Coolant passage at nozzle throat.

APPENDIX D

Numerical Methods of Solution

Flow Analysis. Local Mach number is an implicit function of local area divided by throat area:

$$\frac{A}{A^*} = \frac{1}{Ma} \frac{(1 + 0.2\ Ma^2)^3}{1.728} \quad . \tag{D1}$$

Equation D1 applies to air with $\gamma = 1.4$. Local area is a function of local radius using $A = \pi r^2$. Local radius a function of axial distance is available to the FORTRAN code as a subroutine. Mach number as a function of axial distance is therefore obtained by solving Equation D1 using a numerical regula falsi technique. With a solution for local Mach number, local free stream temperature and pressure are available from compressible flow theory:

$$T_\infty = \frac{T_0}{1 + 0.2\ Ma^2} \quad , \tag{D2}$$

$$P_\infty = P_0\ (1 + 0.2\ Ma^2)^{-3.5} \quad . \tag{D3}$$

Thermal Analysis. A method of successive substitution is required for the thermal analysis in the cooled portion of the nozzle. An initial value is obtained for $T_{w,c}$ using

Equation 8 of the main text and initial guesses for h_c and $T_{w,a}$. The guess for h_c can now be updated using Equation 6 from the main text. Furthermore, $T_{w,a}$ can now be solved for using the new estimate for $T_{w,c}$ and a guessed value for h_a in Equation 7. If the new estimate for $T_{w,a}$ is significantly different from the current estimate, then it becomes the current estimate. The process is repeated starting with a solution for $T_{w,c}$ using the new estimate for h_c. The new estimate for $T_{w,a}$ is significantly different form the current estimate if it differs by more than one degree Celsius.

Note that this successive substitution scheme does not modify h_a. Once $T_{w,a}$ has converged we begin another loop. The air side wall temperature is now used to calculate a new value of h_a with Equation 5. If this new h_a differs from the current value by more than one watt/m^2.°C, then it becomes the current value. The loop that solves for $T_{w,a}$ is repeated first; then h_a is retested. When h_a finally converges we have the air side wall temperature and heat transfer coefficient, and the coolant side wall temperature and heat transfer coefficient as a function of axial position.

Stress Analysis. Equations 10 through 19 in the main text deal with the stress analysis. The ΔT used in Equation 10 and Equation 12 is the difference between air and coolant side wall temperatures. We have those temperatures from the thermal analysis. Also needed is the local free stream air

pressure. This was obtained from the flow analysis. The stress analysis is therefore a relatively straight forward application of Equations 10 through 19.

The FORTRAN code flow chart is given in Figure D1. The code listing is given at the end of this appendix.

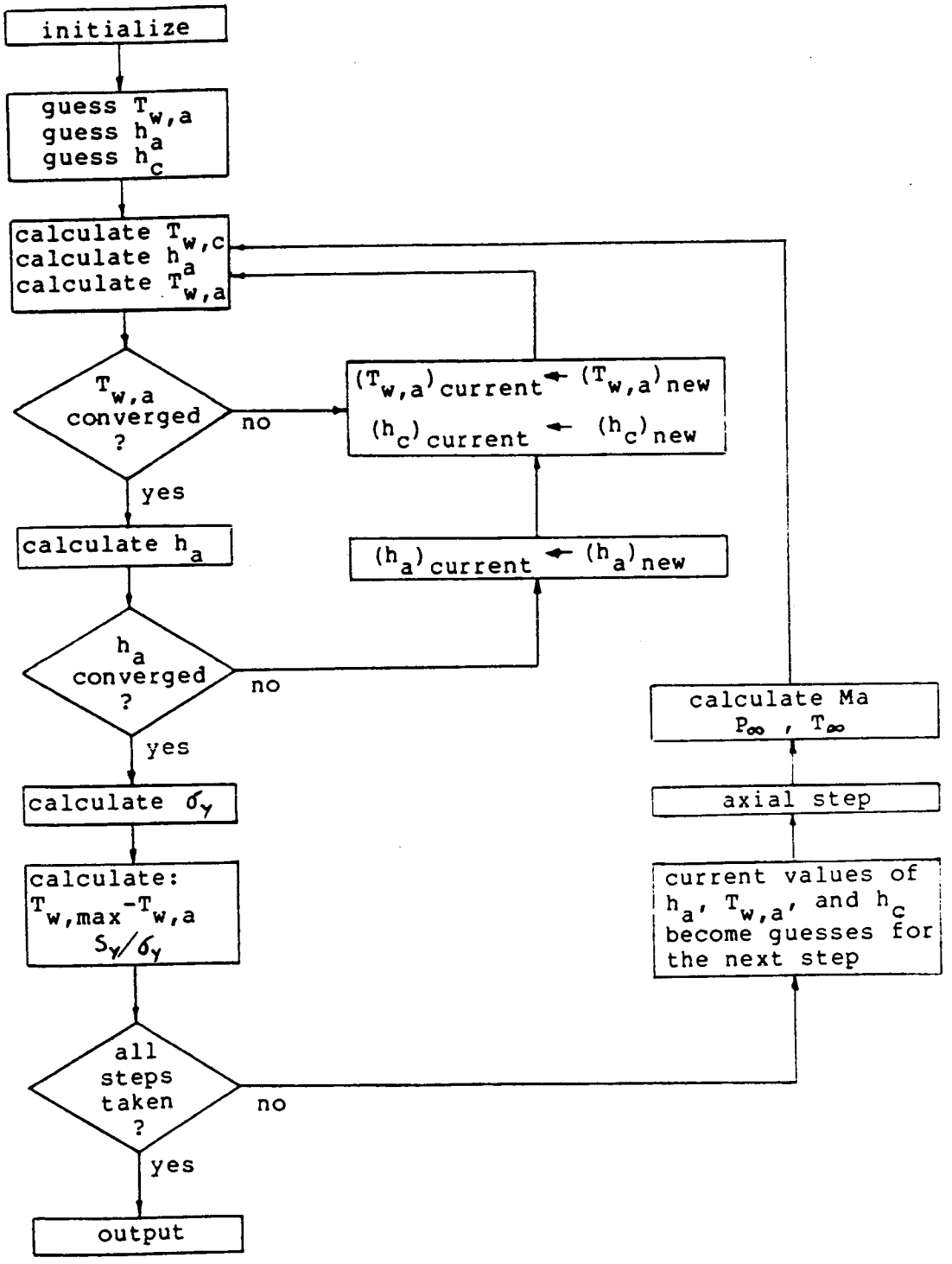

Figure D1. FORTRAN Code Flow Chart.

FORTRAN CODE

```
      PROGRAM MOD2

      CHARACTER*100 IDENT
      CHARACTER*50 AGAIN,HALT,RES,METAL,UNITS,TYPE,CYL
      EXTERNAL FMA,TOP,BOT
      COMMON/FT/ST,TR,TW,TO,DRDZ,MA,DELMA,STEP,RAD,CF,DSDTH,TINF,DELTW
      COMMON/AR/AR
      COMMON/COEF/DELP,DH,L,RO,NU,FRIC,R1,X1,X3
      COMMON/DF/DF
      INTEGER STATN,POS,NEG
      REAL MDOT,NU,MA,L,K,MUO,MUAIR,NUM,NTHTA,NPHI
      REAL TWA(-100:85),TWC(-100:85),YLD1(-100:85),YLD2(-100:85)
      REAL HA(-100:85),HC(-100:85),Q(-100:85),QPP(-100:85)
      REAL EA(0:15),AA(0:15),PA(0:15),AK(0:15),YA(0:15)
      REAL TH(10),UMN(10),TBK(10)
      REAL K1,K2,K3,K4
      OPEN(6,FILE='PRN:')
      DF=400.0
*       ^ THIS DIVIDING FACTOR IS USED TO LESSEN THE ROUND OFF ERROR
*         IN FITTING A POLYNOMIAL CURVE TO THE FUNCTIONAL RELATION
*         BETWEEN THE MATERIAL PROPERTIES AND TEMPERATURE

      DO 3 I=0,15
      EA(I)=0.0
      AA(I)=0.0
      PA(I)=0.0
      AK(I)=0.0
      YA(I)=0.0
    3 CONTINUE

  555 CONTINUE
      CALL DATAIN(EA,AA,PA,AK,YA,METAL)
      PC=13.7895E6
*             ^ PA -- COOLANT PRESSURE (2000 PSI)
  554 CONTINUE
 4321 CONTINUE
      PRINT*,' IDENTIFIER:  '
      READ'(A)',IDENT

      DISTC=1.0
      TMPC=1.0
      VELC=1.0
      HCNV=1.0

      DNSTR=0.12
      DNTHK=0.004
      UPSTR=0.10
      UPTHK=0.004
      X3=0.004
      X2=0.08

      TO=3460.0
      TO=TO/1.8
```

```
      PO=2000.0
      PO=PO*6894.8

      TCRIT=760.0
      TCRIT=TCRIT+273.0

5432  PRINT*,' ENTER "S" FOR SINGLE RUN OR "P" FOR PARAMETRIC OUTPUT '
      READ'(A)',TYPE
      IF (TYPE .EQ. 'P')THEN

      PRINT*,' NUMBER OF THROAT THICKNESSES TO BE TESTED:  '
      READ*,N1
      IF (UNITS .NE. 'EN')THEN
      PRINT*,' ENTER THICKNESS IN METERS  '
      ELSE
      PRINT*,' ENTER THICKNESS IN INCHES  '
      ENDIF
      DO 31 I=1,N1
      PRINT*,' ENTER THICKNESS',I,':  '
   31 READ*,TH(I)

      PRINT*,' NUMBER OF COOLANT SPEEDS TO BE TESTED:  '
      READ*,N2
      IF (UNITS .NE. 'EN')THEN
      PRINT*,' ENTER SPEED IN METERS/SECOND '
      ELSE
      PRINT*,' ENTER SPEED IN FEET/SECOND '
      ENDIF
      DO 32 I=1,N2
      PRINT*,' ENTER SPEED',I,':  '
   32 READ*,UMN(I)

      PRINT*,' NUMBER OF COOLANT BULK TEMPERATURES TO BE TESTED:  '
      READ*,N3
      IF (UNITS .NE. 'EN')THEN
      PRINT*,' ENTER TEMPERATURE IN KELVIN '
      ELSE
      PRINT*,' ENTER TEMPERATURE IN RANKINE '
      ENDIF
      DO 33 I=1,N3
      PRINT*,' ENTER TEMP.',I,':  '
   33 READ*,TBK(I)

      PRINT*,' REPEAT INPUT CYCLE (Y/N)? '
      READ'(A)',AGAIN
      IF(AGAIN .EQ. 'Y')GO TO 554

      ELSE
      PRINT*,' LINER THICKNESS AT THROAT'
      IF (UNITS .NE. 'EN')THEN
      PRINT*,' ENTER THICKNESS IN METERS: '
      ELSE
      PRINT*,' ENTER THICKNESS IN INCHES: '
      ENDIF
      READ*,THTHK
      THTHK=THTHK*DISTC
```

```
      PRINT*,' AVERAGE COOLANT SPEED AT THE THROAT'
      IF (UNITS .NE. 'EN')THEN
      PRINT*,' ENTER SPEED IN METERS/SECOND: '
      ELSE
      PRINT*,' ENTER SPEED IN FEET/SECOND: '
      ENDIF
      READ*,UMT
      UMT=UMT*VELC

      PRINT*,' COOLANT BULK TEMPERATURE'
      IF (UNITS .NE. 'EN')THEN
      PRINT*,' ENTER TEMPERATURE IN KELVIN: '
      ELSE
      PRINT*,' ENTER TEMPERATURE IN RANKINE: '
      ENDIF
      READ*,TB
      TB=TB*TMPC
      PRINT*,' REPEAT INPUT CYCLE (Y/N)? '
      READ'(A)',AGAIN
      IF(AGAIN .EQ. 'Y')GO TO 554
      GO TO 6543

      ENDIF

      DO 20 IT=1,N1
      THTHK=TH(IT)
      DO 21 IB=1,N3
      TB=TBK(IB)
      DO 22 IU=1,N2
      UMT=UMN(IU)

6543  CONTINUE
      DO 5 I=-100,85
      TWA(I)=0.0
      TWC(I)=0.0
      YLD1(I)=0.0
      YLD2(I)=0.0
      HA(I)=0.0
      HC(I)=0.0
   5  CONTINUE

      TOL=0.0
      PI=3.1415926
      GAM=1.4
      RTH=0.224*.0254
*                    ^ METERS -- THROAT DIA.

      STEP=0.0025
      RAD=RADIUS(-0.235)
      HA(-48)=1200.0
      HC(-48)=50000.0
      TWA(-48)=500.0
      TM=430.0
      AR=RAD*RAD/RTH/RTH
      R1=RAD/COS(ATAN((RAD-RADIUS(-0.105))/STEP))
```

```
      CALL SOLVE(1.0E-9,1.0,0.001,500,MA,FMA)
      TINF=TO/(1.0+0.2*MA*MA)
      TR=TINF+0.87*(TO-TINF)
      PINF=PO*(TINF/TO)**3.5
      UAIR=MA*20.0*TINF**0.5
      TWA(-94)=TR

      EPS1=1.0
      EPS2=1.0
      EPS3=.00001
      EPS4=1.0E-10
      EPS5=1.0E-5

      TBR=1.8*TB

**  PROPERTIES OF WATER OVER APPLICABLE RANGE
      CK=0.4483+0.05022*LOG(TB-273.0)
      CRO=1001.5-0.2217*(TB-273.0)
      CPR=133.4*(TB-273.0)**(-0.9354)
      CMU=0.0254*(TB-273.0)**(-0.9828)

      SPC=4200.0
      NU=CMU/CRO
      L=PI*(RTH+THTHK+X3/2.0)
      AREA=X2*X3
      PER=2.0*(X2+X3)
      DH=4.0*AREA/PER
      RE=UMT*DH/NU

      MDOT=2.0*CRO*AREA*UMT
*       ^    THIS IS THE TOTAL MDOT (TOP AND BOTTOM CHANNELS)
      UPBGN=0.0254
      DNBGN=0.0381
      PHI=0.00001
      THTA=0.00001

**********  DO 10 INCREMENTS THE AXIAL POSITION IN THE NOZZLE  ****
      DO 10 STATN=-93,4

      AX=STEP*STATN

      IF (STATN .LT. -16)THEN
      X1=.004-(48+STATN)/400.0*(.004-THTHK)/0.08
      ELSE IF (STATN .GT. 16)THEN
      X1=THTHK+(STATN-16)/400.0*(0.004-THTHK)/0.08
      ELSE
      X1=THTHK
      ENDIF

      ROLD=RAD
      RAD=RADIUS(AX)
      AR=RAD*RAD/RTH/RTH
      R1=RAD/COS(ATAN((RAD-ROLD)/STEP))
      RM=R1+X1/2.0
      R2=R1+X1
```

```
      DELR=RAD-ROLD
      DRDZ=DELR/STEP
      DELX=(STEP**2+DELR**2)**0.5
      X=X+DELX

      OLDMA=MA
      IF (STATN .GE. 0) THEN
      XA=1.0
      XC=16.0
      ELSE
      XA=0.00001
      XC=1.0
      ENDIF
      CALL SOLVE (XA,XC,.001,500,MA,FMA)

      TINF=TO/(1.0+0.2*MA*MA)
      PINF=PO*(TINF/TO)**3.5
      TR=TINF+0.87*(TO-TINF)
       ^ RECOVERY TEMP. -- ALL UNITS ARE SI COMPATIBLE
      UAIR=MA*20.0*TINF**0.5
      DELMA=MA-OLDMA

      ROAIR=PINF/TINF/287.0
      CPAIR=(0.93608+0.00019834*TINF)*1000.0
      MUAIR=(0.05131*TINF**0.63684)*0.00001
      PRAIR=0.78145-0.01169*LOG(TINF)

********* THERMAL ANALYSIS  ********

      IF(STATN .LT. -48)THEN
      TWA(STATN)=TR
      TW=TR
      DELTW=TWA(STATN)-TWA(STATN-1)
      NUM=TRAP(TOP,0.0,1.0,100)
      DENOM=ROMB(BOT,0.0,1.0,5,EPS5,0)

      DSDTH=(1.-7.*TINF*NUM/TWA(STATN))/(7.*TINF*DENOM/TWA(STATN))
      RET=ROAIR*UAIR*THTA/MUAIR
      CF=0.0256*RET**(-0.25)*(0.5*(TWA(STATN)/TINF+1.0))**(-0.6)

      K1=FTHTA(THTA)
      K2=FTHTA(THTA+0.5*STEP*K1)
      K3=FTHTA(THTA+0.5*STEP*K2)
      K4=FTHTA(THTA+STEP*K3)
      THTA=THTA+STEP/6.0*(K1+2.0*K2+2.0*K3+K4)

      K1=F1PHI(PHI)
      K2=F1PHI(PHI+0.5*STEP*K1)
      K3=F1PHI(PHI+0.5*STEP*K2)
      K4=F1PHI(PHI+STEP*K3)
      PHI=PHI+STEP/6.0*(K1+2.0*K2+2.0*K3+K4)

      ELSE
```

```
      K=YY(TM,AK)
   15 CONTINUE
      TWC(STATN)=(K*TWA(STATN)/LOG(R2/R1)+HC(STATN)*R2*TB)/
     & (HC(STATN)*R2+K/LOG(R2/R1))
      TBR=1.8*TB

      YMU=0.0254*(TWC(STATN)-273.0)**(-0.9828)

      HC(STATN)=0.0216*CK*(UM*CRO)**0.8*CPR**(.33333333)/(CMU**0.8*
     & DH**0.2)*(CMU/YMU)**0.14
      RE=UM*DH/NU

      TM=(TWC(STATN)+TWA(STATN))/2.0
      K=YY(TM,AK)
      TWAN=(HA(STATN)*R1*TR+K*TWC(STATN)/LOG(R2/R1))/
     & (K/LOG(R2/R1)+HA(STATN)*R1)
      IF(ABS(TWAN-TWA(STATN)) .GT. EPS1)THEN
      TWA(STATN)=TWAN
      GO TO 15
      ENDIF
      TWA(STATN)=TWAN

      DELTW=TWA(STATN)-TWA(STATN-1)
      TW=TWA(STATN)
      NUM=TRAP(TOP,0.0,1.0,100)
      DENOM=ROMB(BOT,0.0,1.0,5,EPS5,0)
      DSDTH=(1.-7.*TINF*NUM/TWA(STATN))/(7.*TINF*DENOM/TWA(STATN))
      RET=ROAIR*UAIR*THTA/MUAIR
      CF=0.0256*RET**(-0.25)*(0.5*(TWA(STATN)/TINF+1.0))**(-0.6)

      K1=FTHTA(THTA)
      K2=FTHTA(THTA+0.5*STEP*K1)
      K3=FTHTA(THTA+0.5*STEP*K2)
      K4=FTHTA(THTA+STEP*K3)
      THTA=THTA+STEP/6.0*(K1+2.0*K2+2.0*K3+K4)

      ST=(PHI/THTA)**(-0.1)*CF/2.0/(1.0-5.0*(CF/2.0)**0.5*
     & (1.0-PRAIR+LOG(6.0/(5.0*PRAIR+1.0))))

      K1=F2PHI(PHI)
      K2=F2PHI(PHI+0.5*STEP*K1)
      K3=F2PHI(PHI+0.5*STEP*K2)
      K4=F2PHI(PHI+STEP*K3)
      PHI=PHI+STEP/6.0*(K1+2.0*K2+2.0*K3+K4)

      HAN=ST*ROAIR*CPAIR*UAIR

      IF(ABS(HAN-HA(STATN)) .GT. EPS2) THEN
      HA(STATN)=HAN

      GO TO 15
      ENDIF
      ENDIF

      HA(STATN)=HAN
```

```
      DELTAT=TWA(STATN)-TWC(STATN)
      TWC(STATN+1)=TWC(STATN)
      TWA(STATN+1)=TWA(STATN)
      HC(STATN+1)=HC(STATN)
      HA(STATN+1)=HA(STATN)

********** STRESS ANALYSIS **********

      DR=R2*R2-R1*R1

      F1R2=YY(TWA(STATN),AA)*YY(TWA(STATN),EA)*DELTAT*
     & (1.-2.*R2*R2*LOG(R2/R1)/DR)/
     & (2.*(1.-YY(TWA(STATN),PA))*LOG(R2/R1))

      STH1=F1R2+PINF*(R2*R2+R1*R1)/DR-2.*PC*R2*R2/DR
      SZ1=F1R2
      SR1=-PINF

      F1R1=YY(TWA(STATN),AA)*YY(TWA(STATN),EA)*DELTAT*
     & (1.-2.*R1*R1*LOG(R2/R1)/DR)/
     & (2.*(1.-YY(TWA(STATN),PA))*LOG(R2/R1))

      STH2=-F1R1+2.0*PINF*R1*R1/DR-PC*(R2*R2+R1*R1)/DR
      SZ2=-F1R1
      SR2=-PC


      YLD1(STATN)=(.5*((STH1-SR1)**2+(STH1-SZ1)**2+(SZ1-SR1)**2))**.5
      YLD2(STATN)=(.5*((STH2-SR2)**2+(STH2-SZ2)**2+(SZ2-SR2)**2))**.5

******   LOCAL HEAT TRANSFER Q FOR COOLED PORTION OF NOZZLE

      Q(STATN)=2.0*PI*RAD*ABS(STEP)*HC(STATN)*(TWC(STATN)-TB)
      QPP(STATN)=HC(STATN)*(TWC(STATN)-TB)

************** LOOP 10 **************

   10 CONTINUE

      STEP=0.000125

***************   DO 11    ****************

      DO 11 STATN=5,85

      AX=STEP*STATN+0.01
      X1=THTHK
      UM=UMT

      ROLD=RAD
      RAD=RADIUS(AX)
      AR=RAD*RAD/RTH/RTH
      R1=RAD/COS(ATAN((RAD-ROLD)/STEP))
      RM=R1+X1/2.0
      R2=R1+X1
```

```
      DELR=RAD-ROLD
      DRDZ=DELR/STEP
      DELX=(STEP**2+DELR**2)**0.5
      X=X+DELX

      OLDMA=MA
      IF (STATN .GE. 0) THEN
      XA=1.0
      XC=16.0
      ELSE
      XA=0.00001
      XC=1.0
      ENDIF
      CALL SOLVE (XA,XC,.001,500,MA,FMA)

      TINF=TO/(1.0+0.2*MA*MA)
      PINF=PO*(TINF/TO)**3.5
      TR=TINF+0.87*(TO-TINF)
*      ^ RECOVERY TEMP. -- ALL UNITS ARE SI COMPATIBLE
      UAIR=MA*20.0*TINF**0.5
      DELMA=MA-OLDMA

      ROAIR=PINF/TINF/287.0
      CPAIR=(0.93608+0.00019834*TINF)*1000.0
      MUAIR=(0.05131*TINF**0.63684)*0.00001
      PRAIR=0.78145-0.01169*LOG(TINF)

********* THERMAL ANALYSIS  (11) ********

      K=YY(TM,AK)
   16 CONTINUE
      TWC(STATN)=(K*TWA(STATN)/LOG(R2/R1)+HC(STATN)*R2*TB)/
     & (HC(STATN)*R2+K/LOG(R2/R1))
      TBR=1.8*TB
      YMU=0.0254*(TWC(STATN)-273.0)**(-0.9828)
      HC(STATN)=0.0216*CK*(UM*CRO)**0.8*CPR**(.33333333)/(CMU**0.8*
     & DH**0.2)*(CMU/YMU)**0.14
      RE=UM*DH/NU
      TM=(TWC(STATN)+TWA(STATN))/2.0
      K=YY(TM,AK)
      TWAN=(HA(STATN)*R1*TR+K*TWC(STATN)/LOG(R2/R1))/
     & (K/LOG(R2/R1)+HA(STATN)*R1)
      IF(ABS(TWAN-TWA(STATN)) .GT. EPS1)THEN
      TWA(STATN)=TWAN
      GO TO 16
      ENDIF
      TWA(STATN)=TWAN
      DELTW=TWA(STATN)-TWA(STATN-1)
      TW=TWA(STATN)
      NUM=TRAP(TOP,0.0,1.0,100)
      DENOM=ROMB(BOT,0.0,1.0,5,EPS5,0)
      DSDTH=(1.-7.*TINF*NUM/TWA(STATN))/(7.*TINF*DENOM/TWA(STATN))
      RET=ROAIR*UAIR*THTA/MUAIR
      CF=0.0256*RET**(-0.25)*(0.5*(TWA(STATN)/TINF+1.0))**(-0.6)
```

```
      K1=FTHTA(THTA)
      K2=FTHTA(THTA+0.5*STEP*K1)
      K3=FTHTA(THTA+0.5*STEP*K2)
      K4=FTHTA(THTA+STEP*K3)
      THTA=THTA+STEP/6.0*(K1+2.0*K2+2.0*K3+K4)

      ST=(PHI/THTA)**(-0.1)*CF/2.0/(1.0-5.0*(CF/2.0)**0.5*
     & (1.0-PRAIR+LOG(6.0/(5.0*PRAIR+1.0))))

      K1=F2PHI(PHI)
      K2=F2PHI(PHI+0.5*STEP*K1)
      K3=F2PHI(PHI+0.5*STEP*K2)
      K4=F2PHI(PHI+STEP*K3)
      PHI=PHI+STEP/6.0*(K1+2.0*K2+2.0*K3+K4)

      HAN=ST*ROAIR*CPAIR*UAIR

      IF(ABS(HAN-HA(STATN)) .GT. EPS2) THEN
      HA(STATN)=HAN

      GO TO 16
      ENDIF

      HA(STATN)=HAN

      DELTAT=TWA(STATN)-TWC(STATN)
      TWC(STATN+1)=TWC(STATN)
      TWA(STATN+1)=TWA(STATN)
      HC(STATN+1)=HC(STATN)
      HA(STATN+1)=HA(STATN)

********** STRESS ANALYSIS **********

      DR=R2*R2-R1*R1
      F1R2=YY(TWA(STATN),AA)*YY(TWA(STATN),EA)*DELTAT*
     & (1.-2.*R2*R2*LOG(R2/R1)/DR)/
     & (2.*(1.-YY(TWA(STATN),PA))*LOG(R2/R1))
      STH1=F1R2+PINF*(R2*R2+R1*R1)/DR-2.*PC*R2*R2/DR
      SZ1=F1R2
      SR1=-PINF
      F1R1=YY(TWA(STATN),AA)*YY(TWA(STATN),EA)*DELTAT*
     & (1.-2.*R1*R1*LOG(R2/R1)/DR)/
     & (2.*(1.-YY(TWA(STATN),PA))*LOG(R2/R1))
      STH2=-F1R1+2.0*PINF*R1*R1/DR-PC*(R2*R2+R1*R1)/DR
      SZ2=-F1R1
      SR2=-PC
      YLD1(STATN)=(.5*((STH1-SR1)**2+(STH1-SZ1)**2+(SZ1-SR1)**2))**.5
      YLD2(STATN)=(.5*((STH2-SR2)**2+(STH2-SZ2)**2+(SZ2-SR2)**2))**.5

******   LOCAL HEAT TRANSFER Q FOR COOLED PORTION OF NOZZLE
      Q(STATN)=2.0*PI*RAD*ABS(STEP)*HC(STATN)*(TWC(STATN)-TB)
      QPP(STATN)=HC(STATN)*(TWC(STATN)-TB)

************** LOOP 11 **************

   11 CONTINUE
```

```
**********  EQUATIONS MAKING USE OF THE LOCAL HEAT TRANSFER Q

      WRITE(6,800)IDENT
  800 FORMAT(5X,A/)
      WRITE(6,801)METAL
  801 FORMAT(5X,'MATERIAL IS  ',A//)

************   BLOCK J  ************

      WRITE(6,502)
  502 FORMAT ('     LOC      TWA     TWC    FSA    FSC        HA',7X,'HC'
     & ,8X,'QPP        MSA')
      DO 57 I=-28,4
      XLOC=I/4.0
      TMAR=TCRIT-TWA(I)
      FN1=YY(TWA(I),YA)
      FD1=YLD1(I)
      FF1=FN1/FD1
      FN2=YY(TWC(I),YA)
      FD2=YLD2(I)
      FF2=FN2/FD2
      IF(I .GE. -5 .AND. I .LE. 4)THEN
      PRINT*,' SY= ',FN1
      PRINT*,' LOCAL STRESS= ',FD1
      PRINT*,' F.S.= ',FN1/FD1
      ENDIF
      WRITE(6,500)XLOC,TWA(I)/TMPC,TWC(I)/TMPC,FF1,
     & FF2,HA(I)*HCNV,HC(I)*HCNV,QPP(I),TMAR
***               ENGLISH UNITS FOR HTXFR COEFF ARE BTU/(HR*F*FT2)
   57 CONTINUE
  500 FORMAT (1X,F7.2,F8.1,F7.1,2F6.2,2F10.1,F12.1,F8.2)
      DO 58 I=25,85,20
      XLOC=(I-5)/80.0+1.0
      TMAR=TCRIT-TWA(I)
      WRITE(6,500)XLOC,TWA(I)/TMPC,TWC(I)/TMPC,YY(TWA(I),YA)/YLD1(I),
     & YY(TWC(I),YA)/YLD2(I),HA(I)*HCNV,HC(I)*HCNV,QPP(I),TMAR
   58 CONTINUE
      WRITE(6,501)THTHK,UMT,TB
  501 FORMAT (//'  THTHK= ',F6.4,4X,'UMT= ',F4.1,4X,'TB= ',F5.1)
      WRITE(6,903)
  903 FORMAT('1')
      IF(TYPE .NE. 'P') GO TO 1234
   22 CONTINUE
   21 CONTINUE
   20 CONTINUE
 1234 PRINT*,' R=REPEAT W/ SAME MAT''L   N=NEW MAT''L   Q: '
      READ'(A)',RES
      IF(RES .EQ. 'R')THEN
      GO TO 554
      ELSE IF (RES .EQ. 'N')THEN
      GO TO 555
      ENDIF

 1000 END
```

```
******* SUBPROGRAM *******

      SUBROUTINE DATAIN (EA,AA,PA,AK,YA,METAL)
      REAL K,TMP(50),EMP(50),EA(0:15),AA(0:15),PA(0:15),AK(0:15),
     & YA(0:15),AMP(50),PMP(50),AKP(50),YMP(50)
      CHARACTER*50  METAL, NAME, JUNK(2), RES,FORMER,NAM
      FORMER='START'
 101  PRINT*,' ENTER MATERIAL NAME: '
      READ'(A)',METAL
   1  CLOSE(9)
      CLOSE(10)
      CLOSE (11)
      CLOSE  (12)
      CLOSE (14)
      CLOSE(15)
      OPEN(9,FILE='MLIST',STATUS='OLD')
      OPEN(10,FILE='MLIST',STATUS='OLD')
      OPEN(11,FILE='HOLD',STATUS='OLD')
      OPEN(12,FILE='HOLD',STATUS='OLD')
      OPEN(14,FILE='CHOICE')
      OPEN(15,FILE='CHOICE')
      REWIND 9
      READ(9,'(A)')(JUNK(I),I=1,1)
      DO 2 I=1,100
      READ(9,700,END=3)NAME
      WRITE(12,701)NAME
      IF(FORMER .EQ. '%')THEN
      WRITE(15,701)NAME
      ENDIF
      FORMER=NAME
  700 FORMAT (1X,A)
  701 FORMAT (2X,A)
      IF (NAME .EQ. METAL) GO TO 5
    2 CONTINUE
    3 PRINT*,' LIST OF AVAILABLE MATERIALS'
      REWIND 14
      READ(14,'(A)')(JUNK(J),J=1,1)
      DO 30 I=1,100
      READ (14,700,END=31)NAM
   30 WRITE(*,701)NAM
   31 PRINT*,' R=RETRY,  N=ENTER NEW MATERIAL,  Q=QUIT'
      PRINT*,' FOLLOW YOUR SELECTION WITH A CARRAIGE RETURN  '
      READ'(A)',RES
      IF (RES .EQ. 'R' ) THEN
      GO TO 101
      ELSE IF (RES .EQ. 'Q')THEN
      STOP
      ENDIF
      WRITE(12,701)METAL
      PRINT*,' YOUNG''S MODULUS SECTION'
    6 PRINT*,' INPUT TEMP. (-1 TO EXIT)  '
      READ*,TMPK
      IF(TMPK .LT. 0) GO TO 8
      PRINT*,' INPUT YOUNG''S MODULUS  '
      READ*, EL
      WRITE (12,800) TMPK,EL
```

```
800   FORMAT (2X,F6.1,E20.9)
      GO TO 6
  8   WRITE (12,801)'COEFFICIENT OF THERMAL EXPANSION'
801   FORMAT (2X,A)
      PRINT*,' COEFFICIENT OF THERMAL EXPANSION SECTION'
  9   PRINT*,' INPUT TEMP. (-1 TO EXIT)  '
      READ*,TMPK
      IF(TMPK .LT. 0) GO TO 10
      PRINT*,' INPUT COEFFICIENT OF THERMAL EXPANSION  '
      READ*, AL
      WRITE (12,800) TMPK,AL
      GO TO 9
 10   WRITE (12,801)'POISSON RATIO'
      PRINT*,' POISSON RATIO SECTION'
 11   PRINT*,' INPUT TEMP. (-1 TO EXIT)  '
      READ*,TMPK
      IF(TMPK .LT. 0) GO TO 12
      PRINT*,' INPUT POISSON RATIO  '
      READ*, PR
      WRITE (12,800) TMPK,PR
      GO TO 11
 12   WRITE (12,801)'THERMAL CONDUCTIVITY'
      PRINT*,' THERMAL CONDUCTIVITY SECTION'
 14   PRINT*,' INPUT TEMP. (-1 TO EXIT)  '
      READ*,TMPK
      IF(TMPK .LT. 0) GO TO 15
      PRINT*,' INPUT THERMAL CONDUCTIVITY K  '
      READ*, K
      WRITE (12,800) TMPK,K
      GO TO 14
 15   WRITE (12,801)'YIELD STRENGTH'
      PRINT*,' YIELD STRENGTH SECTION'
 16   PRINT*,' INPUT TEMP. (-1 TO EXIT)  '
      READ*,TMPK
      IF(TMPK .LT. 0) GO TO 17
      PRINT*,' INPUT YIELD STRENGTH  '
      READ*, YS
      WRITE (12,800) TMPK,YS
      GO TO 16
 17   WRITE (12,801)'%'

      REWIND 11
      READ(11,'(A)')(JUNK(I),I=1,1)
      DO 7 I=1,100
      READ(11,700,END=1) NAME
      WRITE(10,701)NAME
  7   CONTINUE
      PRINT*,' FILE LENGTH EXCEEDS DO LOOP LIMIT'
      GO TO 1
  5   CONTINUE
      DO 20 I=1,50
      READ(9,802,ERR=21)TMP(I),EMP(I)
 20   CONTINUE
802   FORMAT (1X,F6.1,E20.9)
 21   CONTINUE
      CALL TEMP (TMP,EMP,I-1,EA)
```

```
      DO 22 I=1,50
      READ(9,802,ERR=23)TMP(I),AMP(I)
   22 CONTINUE
   23 CALL TEMP(TMP,AMP,I-1,AA)

      DO 24 I=1,50
      READ(9,802,ERR=25)TMP(I),PMP(I)
   24 CONTINUE
   25 CALL TEMP(TMP,PMP,I-1,PA)

      DO 26 I=1,50
      READ(9,802,ERR=27)TMP(I),AKP(I)
   26 CONTINUE
   27 CALL TEMP(TMP,AKP,I-1,AK)

      DO 28 I=1,50
      READ(9,802,ERR=29)TMP(I),YMP(I)
   28 CONTINUE
   29 CALL TEMP(TMP,YMP,I-1,YA)

 1000 END

*******  SUBPROGRAM  *******

      SUBROUTINE TEMP(T,P,M,C)
**********  FINDS THE POLYNOMIAL COEFFICIENTS OF UP TO A THIRD
**********  DEGREE POLYNOMIAL FIT TO A MATERIAL PROPERTY VS. TEMP.
**********  USING METHOD OF LEAST SQUARES

      REAL T(50),P(50),A(10,10),SUM1(0:15),B(0:15),C(0:15)
      INTEGER CMAX
      COMMON/DF/DF
      DO 5 I=0,15
      SUM1(I)=0.0
      B(I)=0.0
    5 C(I)=0.0
      IF(M .EQ. 1)THEN
      C(0)=P(1)
      RETURN
      ENDIF
      IF(M .LE. 3)THEN
      CMAX=M
      ELSE
      CMAX=3
      ENDIF
      DO 10 K1=1,(CMAX-1)*2
      DO 10 JJ=1,M
      SUM1(K1)=SUM1(K1)+(T(JJ)/DF)**K1
**          NOTE DIVIDING FACTOR ^
   10 CONTINUE
      DO 20 K2=0,CMAX-1
      DO 20 JJ=1,M
      B(K2)=B(K2)+(T(JJ)/DF)**K2*P(JJ)
**         DIVIDING FACTOR ^
   20 CONTINUE
```

```
      DO 30 I=1,CMAX
      IM=I-1
      DO 30 J=1,CMAX
      A(I,J)=SUM1(IM)
   30 IM=IM+1
      A(1,1)=FLOAT(M)
      NN=10
      CALL GAUSS(A,B,C,NN,CMAX)
      RETURN
      END

******* SUBPROGRAM *******

      SUBROUTINE GAUSS (A,B,X,ND,N)
      REAL A(ND,ND),B(ND),X(ND),AINV(50,50)
      DET=1.0
      DO 1 I=1,N
      DO 1 J=1,N
      IF(I .EQ. J) THEN
      AINV(I,I)=1.0
      ELSE
      AINV(I,J)=0.0
      ENDIF
    1 CONTINUE
      DO 9 IPASS=1,N
      IMX=IPASS
      DO 2 IROW=IPASS,N
      IF (ABS(A(IROW,IPASS)) .GT. ABS(A(IMX,IPASS))) THEN
      IMX=IROW
      ENDIF
    2 CONTINUE
      IF(IMX .NE. IPASS) THEN
      DO 3 ICOL=1,N
      TEMP=AINV(IPASS,ICOL)
      AINV(IPASS,ICOL)=AINV(IMX,ICOL)
      AINV(IMX,ICOL)=TEMP
      IF(ICOL .GE. IPASS)THEN
      TEMP=A(IPASS,ICOL)
      A(IPASS,ICOL)=A(IMX,ICOL)
      A(IMX,ICOL)=TEMP
      ENDIF
    3 CONTINUE
      ENDIF
      PIVOT=A(IPASS,IPASS)
      DET=DET*PIVOT
      IF(DET .EQ. 0.0)THEN
      WRITE(*,10)
      STOP
      ENDIF
      DO 6 ICOL=1,N
      AINV(IPASS,ICOL)=AINV(IPASS,ICOL)/PIVOT
      IF(ICOL .GE. IPASS) THEN
      A(IPASS,ICOL) = A(IPASS,ICOL)/PIVOT
      ENDIF
    6 CONTINUE
```

```
      DO 8 IROW=1,N
      IF(IROW .NE. IPASS) THEN
      FACTOR=A(IROW,IPASS)
      ENDIF
      DO 7 ICOL=1,N
      IF (IROW .NE. IPASS) THEN
      AINV(IROW,ICOL)=AINV(IROW,ICOL)-FACTOR*AINV(IPASS,ICOL)
      A(IROW,ICOL)=A(IROW,ICOL)-FACTOR*A(IPASS,ICOL)
      ENDIF
    7 CONTINUE
    8 CONTINUE
    9 CONTINUE
      DO 4 I=1,N
      X(I)=0.0
      DO 4 J=1,N
    4 X(I)=X(I)+AINV(I,J)*B(J)
      RETURN
   10 FORMAT(5X,'--- ERROR IN GAUSS ---  THE MATRIX IS SINGULAR',/,
     & 10X,'PROGRAM TERMINATED')
      END

******* SUBPROGRAM *******

      FUNCTION YY(T,C)
      REAL C(0:15)
      COMMON/DF/DF
      YY=0.0
      DO 10 I=0,5
    10 YY=YY+C(I)*(T/DF)**I
      END

******* SUBPROGRAM *******

      FUNCTION RADIUS(X)
*  FINDS RADIUS AS FUNCTION OF AXIAL LOCATION
*   DISTANCE MUST BE IN METERS

      XI=X/0.0254
*  CONVERSION TO INCHES

      IF (XI .GE. 1.7) THEN
      RADIUS=(0.2253*XI+0.08199)*.0254
      RETURN
      ELSE IF( XI .LE.- 0.60) THEN
      RADIUS=(-0.39825*XI+0.07705)*0.0254
      RETURN
      ELSE
      XI=XI+0.60
      RADIUS=0.316-.4266*XI+.73*XI*XI-.6132*XI**3+
     & .2828*XI**4-.0273*XI**5-.0231*XI**6+.00587*XI**7
      RADIUS=RADIUS*.0254
      RETURN
      ENDIF
      END
```

```
******  SUBPROGRAM  ******
      SUBROUTINE SOLVE(XA,XC,EPS,IMAX,ROOT,F)
      X1=XA
      X3=XC
      I=0
      F1=F(X1)
      F3=F(X3)
      D=X3-X1
  1   X2=X1-D*F1/(F3-F1)
      F2=F(X2)
      IF(D .LT. EPS) THEN
      ROOT=X2
      ITER=I
      RETURN
      ELSE IF (ABS(F(X2)) .LT. EPS)THEN
      ROOT=X2
      ITER=I
      RETURN
      ELSE IF (I .GT. IMAX) THEN
      WRITE(*,10)I,X2,F2
      STOP
      ENDIF
      IF(F1*F2 .LT. 0.0)THEN
      X3=X2
      F3=F2
      F1=.9*F1
      ELSE IF (F2*F3 .LT. 0.0)THEN
      X1=X2
      F1=F2
      F3=.9*F3
      ELSE
      WRITE(*,*)'NO ROOT IN INTERVAL',X1,X3,'IN STEP',I
      STOP
      ENDIF
      D=X3-X1
      I=I+1
      GOTO 1
  10  FORMAT(5X,'NO ROOT HAS BEEN FOUND IN',I4,'ITERATIONS',/,
     &       5X,'THE LATEST VALUES ARE X= ',F10.5,
     &       ' AND F(X)= ',E11.4)
      END

******  SUBPROGRAM  ******
      FUNCTION FMA(MA)
      COMMON/AR/AR
      REAL MA
      FMA=AR-(1.0+0.2*MA*MA)**3/(1.728*MA)
      END

******  SUBPROGRAM  ******
      FUNCTION ROMB(F,A,B,KMX,EPS,IPRNT)
      REAL T(0:15,0:15),R(0:15,0:15),DX,A,B,EPS,SUM
      INTEGER K,M,NPTS,KMX,IPRNT
      K=0
      DX=(B-A)
      T(0,0)=0.5*DX*(F(A)-F(B))
```

```
    1  K=K+1
       NPTS=2**K
       DX=DX/2
       SUM=0.0
       DO 2 I=1,NPTS-1,2
       SUM=SUM+F(A+I*DX)
    2  CONTINUE
       T(K,0)=T(K-1,0)/2.0+DX*SUM
       DO 3 M=0,K-1
       T(K,M+1)=T(K,M)+(T(K,M)-T(K-1,M))/(4.0**(M+1)-1.0)
       IF(K .GE. 2 .AND. M .LT. K-2)THEN
       R(K,M)=(T(K-1,M)-T(K-2,M))/(T(K,M)-T(K-1,M))/4.0**(M+1)
       IF (ABS(R(K,M)-1.0) .GT. 0.75 )THEN
       WRITE(*,10)R(K,M),T(K-1,K-1)
       IF(IPRNT .EQ.1)GO TO 5
       ROMB=T(K-1,K-1)
       RETURN
       ENDIF
       ENDIF
    3  CONTINUE
       IF(ABS(T(K,K)-T(K-1,K-1)) .LT. EPS)THEN
       ROMB=T(K,K)
       IF(IPRNT .EQ. 1)GO TO 5
       RETURN
       ELSE IF(K .LT. KMX)THEN
       GO TO 1
       ELSE
       WRITE(*,11)KMX,T(K,K),T(K-1,K-1)
       ROMB=T(K,K)
       IF(IPRNT .EQ. 1)GO TO 5
       RETURN
       ENDIF

*       OUTPUT TABLE
    5  CONTINUE
       WRITE(*,12)(I,I=0,K)
       DO 6 I=0,K
       WRITE(*,13)I,(T(I,M),M=0,I)
    6  CONTINUE
       WRITE(*,14)(I,I=0,K)
       DO 7 I=2,K
       WRITE(*,15)I,(R(I,M),M=0,I-2)
    7  CONTINUE
       ROMB=T(K,K)
       RETURN

*    FORMATS
    10 FORMAT(T20,' WARNING FROM ROMBERG INTEGRATION FUNCTION',/,
      +       T20,'ROUND-OFF ERROR FLAG          = ',F9.5,/,
      +       T20,'MOST RECENT DIAG. ROMBERG TERM= ',E12.6,/,
      +       T20,'CALCULATION HALTED AND THIS VALUE RETURNED')

    11 FORMAT(T20,'WARNING FROM ROMBERG INTEGRATION FUNCTION',/,
      +       T20,'THROUGH ORDER ',I2,' THE REQUIRED ACCURACY',/,
      +       T20,'COULD NOT BE ACHIEVED.  THE LATEST VALUE',/,
      +       T20,'RETURNED TO THE CALLING PROGRAM WAS = ',E12.6,/,
```

```
     +       T20,'AND THE PREVIOUS VALUE IN TABLE IS = ',E12.6)
  12 FORMAT(///,T10,'THE ROMBERG TABLE',//,T5,'LEVEL =>',/,
     +       1X,'ORDER',/,1X,9(6X,I2,6X))
  13 FORMAT(1X,I2,1X,9(F13.9,1X))
  14 FORMAT(//,T10,'THE TABLE OF THE ROUND-OFF ERROR FLAGS',//,
     +       T10,'LEVEL =>',/,1X,'ORDER',/,4X,15(3X,I2,3X))
  15 FORMAT(1X,I2,1X,15(F7.4,1X))
     END

******* SUBPROGRAM *******

     FUNCTION TOP(S)
     COMMON/FT/ST,TR,TW,TO,DRDZ,MA,DELMA,STEP,RAD,CF,DSDTH,TINF,DELTW
     B=TO/TW
     C=(TO-TINF)/TW
     TOP=S**7/(1.0+B*S-C*S*S)
     END

******* SUBPROGRAM *******
     FUNCTION BOT(S)
     COMMON/FT/ST,TR,TW,TO,DRDZ,MA,DELMA,STEP,RAD,CF,DSDTH,TINF,DELTW
     B=TO/TW
     C=(TO-TINF)/TW
     BOT=S**7*(1.0-S)/(1.0+B*S-C*S*S)
     END

******* SUBPROGRAM *******
     FUNCTION TRAP (F,A,B,IDV)
     DX=(B-A)/IDV
     X=A
     TERM1=F(X)
     TRAP=0.0
     DO 10 I=0,IDV
     X=X+DX
     TERM2=F(X)
     TRAP=TRAP+0.5*DX*(TERM1+TERM2)
     TERM1=TERM2
  10 CONTINUE
     END

******* SUBPROGRAM *******
     FUNCTION FTHTA(THTA)
     COMMON/FT/ST,TR,TW,TO,DRDZ,MA,DELMA,STEP,RAD,CF,DSDTH,TINF,DELTW
     REAL MA
     FTHTA=CF/2.0*(1.0+DRDZ*DRDZ)**0.5-THTA*
    & ((2.0-MA*MA+DSDTH)/(MA+0.2*MA**3)*DELMA/STEP+DRDZ/RAD)
     END

******* SUBPROGRAM *******
     FUNCTION F1PHI(PHI)
     COMMON/FT/ST,TR,TW,TO,DRDZ,MA,DELMA,STEP,RAD,CF,DSDTH,TINF,DELTW
     REAL MA
     F1PHI=-PHI*(1.0-MA*MA)/(MA+0.2*MA**3)*DELMA/STEP+DRDZ/RAD
    & -DELTW/STEP/(TO-TW)
     END
```

```
******  SUBPROGRAM  ******
      FUNCTION F2PHI(PHI)
      COMMON/FT/ST,TR,TW,TO,DRDZ,MA,DELMA,STEP,RAD,CF,DSDTH,TINF,DELTW
      REAL MA
      F2PHI=ST*((TR-TW)/(TO-TW))*(1.+DRDZ*DRDZ)**.5
     & -PHI*((1.0-MA*MA)/(MA+0.2*MA**3)*DELMA/STEP+DRDZ/RAD
     & -DELTW/STEP/(TO-TW))
      END
```

APPENDIX E

Temperature distribution in the nozzle wall

We can write the general expression for heat transfer through the nozzle liner wall:

$$q_k = \frac{\int_{T_{w,a}}^{T} k(T)\, dT}{\frac{\ln(r_o/r_i)}{2\pi\Delta L}} \quad . \tag{E1}$$

This can be rewritten as

$$q_k \ln(r/r_i) = -k\, 2\pi\Delta L\, (T - T_{w,a}) \quad . \tag{E2}$$

Now solve for T.

$$T - T_{w,a} = \frac{-q_k}{2\pi k\, \Delta L\, \ln r_i} \ln r \quad ;$$

$$\text{let} \quad K = \frac{-q_k}{2\pi k\, \Delta L\, \ln r_i} \quad ;$$

$$\text{then} \quad T = K \ln(r) + T_{w,a} \quad .$$

Thus, the temperature through the nozzle liner wall has been shown to be a logarithmic function of the radial distance.

APPENDIX F

Comparison of Thermal and Pressure Stresses

The highest stresses, and therefore the lowest factors of safety, occur at the throat. It is in this region that we should compare the pressure stresses with the thermal stresses. For the inside surface of the nozzle liner we have thermal stress defined by Equation 10 in the main text. The pressure stress is defined by Equation 14.

At throat conditions for the material TZM with a liner thickness of 1.5 mm we have the following values:

$\alpha = 0.554 \times 10^{-5}$ m/m K

$E = 0.23 \times 10^{12}$ Pa

$T = 400$ Kelvin

$r_i = 0.00569$ m

$r_o = 0.00719$ m

$\lambda = 0.3$

$P = 7.29 \times 10^{6}$ Pa

$P_c = 13.8 \times 10^{6}$ Pa

Using Equations 10 and 14:

$$(\sigma_{\theta,i})_{thermal} = 3.93 \times 10^{8} \quad ,$$

and

$$(\sigma_{\theta,i})_{pressure} = 2.10 \times 10^{7} \quad .$$

The ratio of thermal stress to pressure stress is 18.7. We conclude that the nozzle design will be based largely on thermal stress considerations.

APPENDIX G

Pre-blowdown Nozzle Failure

Before the blowdown process is begun the coolant side of the nozzle liner will be subjected to the full 2000 psi coolant pressure, while the air side will experience a hard vacuum. Two modes of failure must be considered in this case: compressive failure and buckling failure.

Compressive failure. For this analysis we use the same triaxial state of stress treatment used for the operational condition except that we remove thermal stresses and stresses due to air pressure. In this way we can calculate a Factor of Safety. The results of this analysis are shown in Figure F1. It can be seen that the minimum Factor of Safety is 4.18 at the location furthest upstream of the throat. Compressive failure, then, in the pre-blowdown condition is not a problem.

Buckling failure. For this analysis we employ buckling failure theory for a right cylindrical shell. A more accurate model would be to use analysis for a conical shell. However, a cylindrical shell is less resistant to failure than a conical shell, and so we will obtain a very conservative result. If this result is acceptable for a cylinder, we can be quite sure it will be acceptable for a cone.

The equation used for this analysis comes from Faupel [26]:

$$P_{crit} = \frac{E\ t^3}{4\ R^3\ (1 - \lambda^2)} \quad , \qquad \text{(F1)}$$

where R and t are the local nozzle radius and thickness, respectively, and λ is Poisson's ratio. The results of this analysis are shown in Figure F2. The minimum critical pressure for buckling is seen to be 6300 psi. Since 2000 psi is the maximum pressure the liner wall will be subjected to, buckling failure is not a problem.

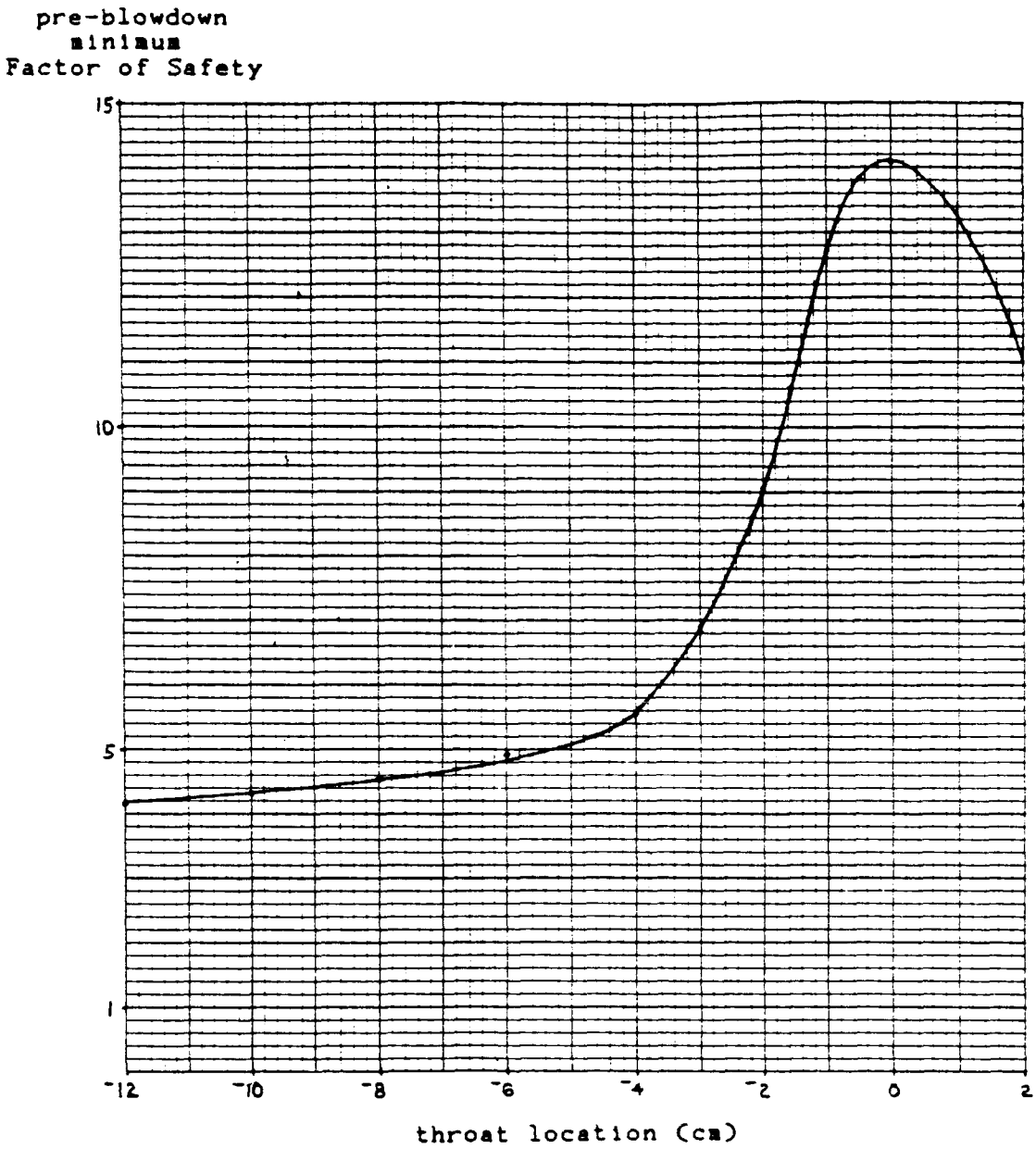

Figure F1. Compressive stress for pre-blowdown condition.

C-2

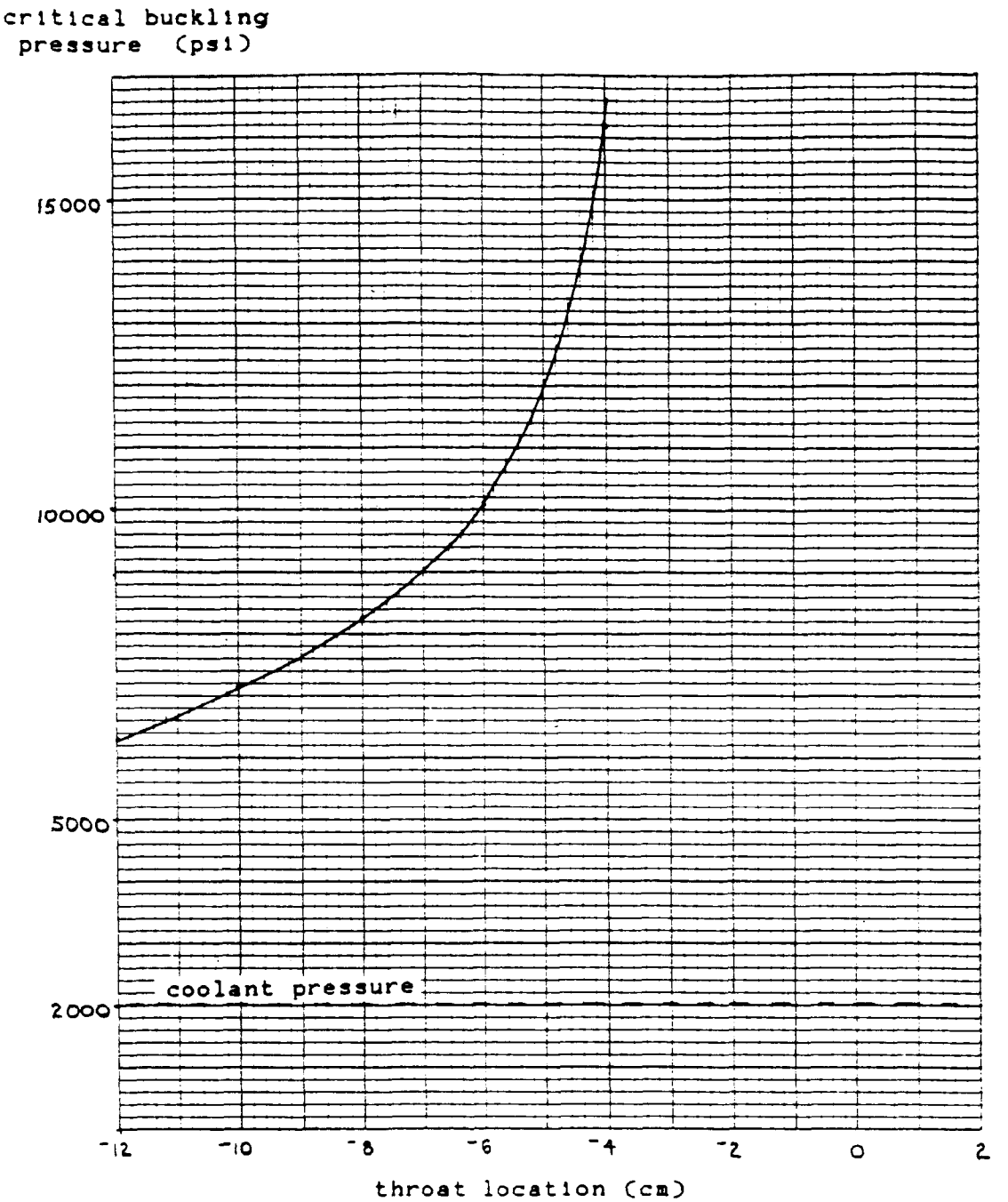

Figure F2. Buckling analysis.